Targeting a mitochondrial E3 ubiquitin ligase complex to overcome AML cell-intrinsic Venetoclax resistance

中尾, 文彦

Targeting a mitochondrial E3 ubiquitin ligase complex to overcome AML cell-intrinsic Venetoclax resistance

Fumihiko Nakao[1], Kiyoko Setoguchi[2], Yuichiro Semba[1], Takuji Yamauchi[1], Jumpei Nogami[1], Kensuke Sasaki[1], Hiroshi Imanaga[1], Tatsuya Terasaki[1], Manaka Miyazaki[2], Shigeki Hirabayashi[2], Kohta Miyawaki[1, 2], Yoshikane Kikushige[1, 3], Takeshi Masuda[4], Koichi Akashi[1, 3] and Takahiro Maeda[2*]

*Corresponding Author

Affiliations [1]Department of Medicine and Biosystemic Science, Kyushu University Graduate School of Medical Sciences, Fukuoka, Japan; [2]Division of Precision Medicine, Kyushu University Graduate School of Medical Sciences, Fukuoka, Japan; [3]Center for Cellular and Molecular Medicine, Kyushu University Hospital, Fukuoka, Japan; [4]Department of Pharmaceutical Microbiology, Faculty of Life Sciences, Kumamoto University, Kumamoto, Japan.

Word counts: 156 (abstract); 4018 (main text)

Figure/table count: 5, Reference count: 57

Abstract

To identify molecules/pathways governing Venetoclax (VEN) sensitivity, we performed genome-wide CRISPR/Cas9 screens using a mouse AML line insensitive to VEN-induced mitochondrial apoptosis. Levels of sgRNAs targeting *March5*, *Ube2j2* or *Ube2k* significantly decreased upon VEN treatment, suggesting synthetic lethal interaction. Depletion of either Ube2j2 or Ube2k sensitized AML cells to VEN only in the presence of March5, suggesting coordinate function of the E2s Ube2j2 and Ube2k with the E3 ligase March5. We next performed CRISPR screens using *March5* knockout cells and identified Noxa as a key March5 substrate. Mechanistically, Bax released from Bcl2 upon VEN treatment was entrapped by Mcl1 and Bcl-XL and failed to induce apoptosis in March5 intact AML cells. By contrast, in *March5* knockout cells, liberated Bax did not bind to Mcl1, as Noxa likely occupied Mcl1 BH3-binding grooves and efficiently induced mitochondrial apoptosis. We reveal molecular mechanisms underlying AML cell-intrinsic VEN resistance and suggest a novel means to sensitize AML cells to VEN.

Introduction

Acute myeloid leukemia (AML) is a devastating disease with a long-term survival rate of less than 30% [1-3]. In recent years, several new anti-AML drugs were FDA-approved and are now widely used in practice; however, more therapeutic options are critically needed, particularly for patients categorized in the adverse-risk group[3] and for those ineligible for intensive chemotherapy (IC) and/or hematopoietic stem cell transplantation [3,4].

Venetoclax (VEN), a BCL2 inhibitor, is among the most promising new drugs for AML therapy due, in part, to its unique mechanisms of action [4-9]. Patients treated with VEN combined with either 5-Azacitidine (Aza) or low dose cytarabine (LD-AraC) exhibit significantly better clinical outcomes than those treated with either Aza or LD-AraC alone [8,10]. While *IDH* mutations are reportedly associated with better response to VEN monotherapy and/or combination therapies [5,6,8], molecular mechanisms regulating VEN sensitivity remain largely unknown.

VEN is a BCL2-specific inhibitor developed based on prototypic small molecules that directly bind to the BH3-binding grooves of anti-apoptotic proteins [11-13]. The current model in the field is that VEN binds to the BCL2 BH3-binding groove, where BAX and other BH3-only proteins reside, releasing BAX from BCL2. Freed BAX then self-assembles and forms pores that permeabilize the mitochondrial outer membrane (MOM). Cytochrome c subsequently released from mitochondria then activates the caspase “death pathway”, leading to cellular apoptosis [14,15].

Although patients harboring *IDH* mutations generally respond positively to VEN-containing therapies, responses among other AML patients vary [5,6,8], and physicians

currently use VEN across the board often without knowing which patients will respond well to VEN therapy. Although novel strategies, such as BH3 profiling [16], have been used to stratify patients for VEN treatment in clinical trial settings, predictive biomarkers of VEN sensitivity are generally unavailable in current practice.

Here we show that in AML cells, the MARCH5 mitochondrial E3 ligase complex, which is comprised of MARCH5, UBE2K, and UBE2J2, regulates VEN sensitivity via modulating BAX saturation of anti-apoptotic proteins.

Results

A genome-wide CRISPR-Cas9 screen identifies components of an E3 ubiquitin ligase complex as modulators of VEN sensitivity

To identify molecules/pathways relevant to VEN sensitivity, we performed genome-wide CRISPR-Cas9 screens in the presence of either DMSO vehicle, VEN or the MCL1 inhibitor S63845 [17] using a mouse AML line (mMA9Cas) that we established (**Fig. 1a** and **Supplemental Fig. 1a**) [18]. Changes in sgRNA abundance before and after the culture period were assessed using the MAGeCK MLE program [19] (**Supplemental Tables 1** and **2**). Both VEN or S63845 treatment dose-dependently suppressed cell growth (**Supplemental Fig. 1b**); however, S63845, but not VEN, induced cellular apoptosis, as evidenced by increased levels of cytosolic cytochrome c (**Supplemental Fig. 1c, d**) and Annexin V (**Supplemental Fig. 1e, f**). Of note, VEN treatment led to increased Annexin V levels at a later time point (18h) in mMA9Cas cells, regardless of *Bax*/*Bak1* status, indicating that VEN induces cell death independently of mitochondrial apoptosis, defined here as spontaneous cell death dependent on Bax and/or Bak1, as reported [20-22] (**Supplemental Fig. 1f**). In fact, the VEN IC50 value in *Bax*/*Bak1* double knockout (DKO) cells was comparable to that seen in WT cells (**Supplemental Fig. 1g**). Furthermore, VEN suppressed proliferation of *Bcl2* KO cells, suggesting that VEN induces cell death, at least in part, through Bcl2-independent mechanisms [22] in mMA9Cas cells (**Supplemental Fig. h**).

As expected, sgRNAs targeting genes encoding factors relevant to mitochondrial apoptosis, such as *Bax*, *Bak1*, *Apaf1* and *Casp9*, were significantly enriched in cells cultured with S63845 (**Fig. 1b**). By contrast, none of those sgRNAs were enriched by

VEN treatment, in agreement with our observation that mMA9Cas cells are resistant to VEN-induced mitochondrial apoptosis (**Fig. 1b, Supplemental Fig. 1c-h**). Interestingly, depletion of either *Ube2j2*, *Ube2k* or *March5*, all of which encode components of a ubiquitin complex, resulted in phenotypes that strongly suggest synthetic lethal interaction with VEN treatment (**Fig. 1b, c**). To validate these findings, we depleted each gene in mMA9Cas cells via lentivirus-based Crimson-tagged sgRNA and assessed effects on cell growth over 9 days with or without VEN. Cells expressing sgRNA targeting either *Ube2j2, Ube2K* or *March5*, but not those transduced with empty vector, demonstrated a proliferative disadvantage relative to non-transduced cells in the presence of VEN (**Fig. 1d**). Importantly, cells lacking any one of the three genes—*Ube2j2, Ube2K* or *March5*—underwent mitochondrial apoptosis upon VEN treatment, as evidenced by increased Annexin V and cleaved caspase 3 levels (**Fig. 1e, f**). We next established mMA9Cas cells lacking either *Ube2j2, Ube2k* or *March5* and then added-back codon-optimized, sgRNA-resistant cDNA corresponding to respective ablated genes using lentiviral vectors also expressing humanized Kusabira Orange 1 (hKO1) fluorescent protein (**Supplemental Fig. 1i**). Proportions of hKO1-positive cells were assessed by FACS over 6 days after VEN treatment. As expected, cells overexpressing each relevant cDNA exhibited a growth advantage over those expressing empty vector in the presence of VEN (**Fig. 1g**). By contrast, overexpression of either Ube2j2, Ube2k or March5 did not alter growth of WT mMA9Cas cells (**Supplemental Fig. 1j**).

March5/Ube2j2/ube2k coordinately regulate VEN sensitivity in AML cells

Since *Ube2j2* and *Ube2k* encode E2 ubiquitin-conjugating enzymes [23,24], we asked whether either functions together with the March5 E3 ligase. To do so, we depleted *March5*-wild type (WT) or -KO mMA9Cas cells of either *Ube2j2* or *Ube2k* via lentivirus-based Crimson-tagged sgRNA and assessed cell growth over 6 days with or without VEN. Deletion of either *Ube2j2* or *Ube2k* enhanced VEN sensitivity in *March5* WT but not *March5* KO cells, suggesting that both Ube2j2 and Ube2k function in a March5-dependent manner (**Fig. 2a**).

RING domain-containing E3 ligases, such as March5, bind both substrates and E2 ubiquitin-conjugating enzymes, facilitating transfer of ubiquitin from the E2 to substrates [25]. The RING domain is required for RING-E2 interaction as well as E3 ubiquitin ligase activity [25]. Thus, we asked whether March5 ligase activity is required to modulate VEN sensitivity. To do so, we added-back either WT or ligase-mutant March5 (H43W or C65/68S) [26] to *March5* KO cells and assessed proportions of transduced cells over time, with or without VEN. Cells expressing WT March5, but not ligase mutants, were VEN-resistant (**Fig. 2b**), suggesting that the March5 E3 ligase and the two E2 enzymes function together to ubiquitinate a substrate (s) relevant to VEN sensitivity (**Fig. 2c**). In fact, results derived from an in vitro glutathione S-transferase (GST)-binding assay indicated direct interaction of March5 with Ube2j2, but not with Ube2k (**Supplemental Fig. 1k, l**).

March5 depletion sensitizes AML cells to VEN and A-1155463

Since *March5* depletion was synthetic lethal to VEN, we next asked whether March5 depletion also sensitizes AML cells to other BH3 mimetics. To do so, we treated

March5-WT and -KO mMA9Cas cells with either VEN, the Bcl-XL inhibitor A-1155463 [27] or the Mcl1 inhibitor S63845 [17] and monitored dose-dependent changes in cell viability. *March5* KO cells were significantly sensitive to VEN and A-1155463, but not to S63845 (**Fig. 3a**). Importantly, mitochondrial apoptosis induced by either VEN or A-1155463 primarily depended on Bax, while apoptosis induced by S63845 was Bak1-dependent (**Supplemental Fig. 2a**). We next asked whether "acute" March5 depletion could sensitize cells to VEN and/or A-1155463 by employing the dTAG system [28,29]. To do so, we established *March5* KO mMA9Cas cells stably expressing HA-FKBP12^{F36V}-tagged March5 (mMA9Cas^{M5FK}) and induced March5 protein degradation via dTag^{V}-1 ligand treatment (**Supplemental Fig. 2b**). dTag^{V}-1 treatment promoted efficient degradation of exogenous March5 protein within 1-3h, as revealed by Western blotting and immunofluorescence analysis (IF) (**Supplemental Fig. 2c, d**). Acute March5 depletion significantly enhanced sensitivity to VEN and A-1155463, as observed in *March5* KO cells (**Fig. 3b**). Importantly, both VEN and A-1155463 induced mitochondrial apoptosis in cells pre-treated with dTag^{V}-1 but not with the negative control ligand dTag^{V}-1-NEG, a diastereomer of dTag^{V}-1 that cannot bind VHL [29]: specifically, we detected cleaved-caspase3 within an hour of VEN or A-1155463 treatment in dTag^{V}-1-pre-treated cells (**Fig. 3c**). Furthermore, Bax localization at mitochondrial membranes, indicative of Bax oligomer formation at the MOM, as well as cytochrome c release from mitochondria were evident upon VEN or A1155463 treatment in cells pre-treated with dTag^{V}-1 (**Fig. 3d** and **Supplemental Fig. 2e**).

We next established human AML lines deficient in endogenous *MARCH5* in which FKBP12^{F36V}-tagged MARCH5 was exogenously expressed. dTag^{V}-1 treatment of

these cells induced MARCH5 degradation dose- and time-dependently (**Supplemental Fig. 2f, g**). Moreover, dTag^{V}-1-mediated MARCH5 depletion significantly enhanced VEN sensitivity in Molm-13, OCI-AML3 and NB-4 lines, while A-1155463 sensitivity was only modestly affected and S63845 sensitivity was unchanged (**Supplemental Fig. 2h**).

Enhanced VEN or A-1155463 sensitivity seen in March5-depleted cells depends on levels of anti-apoptotic proteins

We next asked whether levels of anti-apoptotic proteins affect enhanced sensitivity to BH3 mimetics observed in March5-depleted cells. To do so, we established mMA9Cas^{M5FK} cells overexpressing either Bcl2, Bcl-XL or Mcl1 and generated dose response curves in the presence (dTag^{V}-1-NEG-treated) or absence (dTag^{V}-1-treated) of March5. Strikingly, exogenous expression of either Bcl-XL or Mcl1 completely abolished VEN sensitivity observed upon March5 depletion, while VEN sensitivity was enhanced by Bcl2 overexpression (**Fig. 3e**). Similarly, enhanced sensitivity to A-1155463 observed upon March5 depletion was abolished when either Bcl2 or Mcl1 was overexpressed (**Fig. 3e**). By contrast, S63845 sensitivity was barely altered by overexpression of any of the three anti-apoptotic proteins analyzed (**Fig. 3e**).

Noxa is a substrate of the March5/Ube2j2/Ube2k E3 ubiquitin complex and regulates VEN and A-1155463 sensitivity

To identify a March5 substrate relevant to VEN sensitivity, we performed genome-wide CRISPR/Cas9 screens in the presence or absence of VEN using *March5* KO mMA9Cas cells (**Fig. 4a** and **Supplemental Table 2**). Importantly, neither *Ube2j2* nor *Ube2k* was

synthetic lethal to VEN in *March5* KO cells (**Fig. 4b**), supporting the idea that Ube2j2 and Ube2k function March5-dependently (**Fig. 2a**). While sgRNAs targeting apoptosis-related genes were not enriched by VEN treatment in parental mMA9Cas cells (**Fig. 1b**), sgRNAs targeting *Bax*, *Bak1*, *Apaf1*, *Casp9* and *Pmaip1* were significantly enriched upon VEN treatment of *March5* KO cells (**Fig. 4b**). Since sgRNAs targeting *Pmaip1*, which encodes Noxa, were uniquely enriched in the *March5* KO screen (**Fig. 4b** and **Supplemental Fig. 3a**) but not in the original S63845 screen (**Fig. 1b**), we assessed Noxa protein levels in cells lacking either *March5*, *Ube2j2* or *Ube2k* (**Fig. 4c**). Noxa protein levels robustly increased in *March5* KO cells relative to WT controls and showed moderate increases in *Ube2j2*- or *Ube2k*-KO cells (**Fig. 4c**). Furthermore, Noxa protein was barely detectable in *March5* KO cells overexpressing WT March5 but returned to high levels in cells expressing the March5$^{C65/68S}$ ligase mutant (**Fig. 4c**). Of note, expression levels of Bcl2, Mcl1 and Bcl-XL were comparable among all cells analyzed (**Fig. 4c**). Noxa protein levels were higher in *Ube2j2/Ube2k* DKO cells than in either single KO line, indicative of functional redundancy of these E2s (**Supplemental Fig. 3b**). Noxa protein was upregulated upon dTag^{V}-1-mediated March5 depletion in mMA9Cas^{M5FK} cells, primarily at mitochondria (**Fig. 4d**, **Supplemental Fig. 3c, d**). As expected, treatment of cells with the proteasome inhibitor MG132 enhanced Noxa protein levels to a degree comparable to *March5* KO. By contrast, MG132 treatment had little effect on Noxa protein levels in *March5* KO cells, suggesting that March5 plays a major role in Noxa protein degradation in mMA9Cas cells (**Supplemental Fig. 3e**). While MARCH5 reportedly mediates MCL1 protein degradation [30-32], Mcl1 protein levels were largely unaffected by March5 depletion (**Fig. 4c**, **Supplemental Fig. 3f**). By

contrast, Mcl1 protein levels were significantly enhanced by Noxa depletion (**Supplemental Fig. 3f**), suggesting that E3s other than March5 regulate Mcl1 protein levels Noxa-dependently in mMA9Cas cells.

To determine whether VEN or A1155463 sensitivity "acquired" following March5 depletion depends on Noxa, we established *Pmaip1* KO and *Pmaip1/March5* double KO (DKO) cells (**Supplemental Fig. 3g**), treated them 48h with various doses of VEN or A-1155463 and generated dose response curves. Strikingly, cells subjected to *Pmaip1/March5* DKO were significantly less sensitive to VEN and A-1155463 than were *March5* single KO cells (**Fig. 4e**). Furthermore, *Pmaip1* deletion significantly weakened VEN and A-1155463 sensitivity after $dTag^{V}$-1-mediated March5 depletion (**Supplemental Fig. 3h**). Similarly, VEN sensitivity was decreased by *MARCH5/PMAIP1* depletion in human AML lines (**Supplementary Fig. 3i, j**). As expected, mitochondrial apoptosis, as evidenced by cleaved caspase 3 levels, was not evident following VEN or A-1155463 treatment in March5-depleted cells in the absence of *Pmaip1* (**Fig. 4f**). Thus, we conclude that enhanced VEN or A-1155463 sensitivity observed upon March5 depletion depends primarily on Noxa.

We next assessed potential physical interaction between Noxa and March5. To do so, we performed immunoprecipitation (IP) using *March5* KO mMA9Cas cells stably expressing the Myc-tagged $March5^{C65/68S}$ mutant. IP using anti-Myc or -Noxa antibodies efficiently pulled-down Noxa or Myc-tagged $March5^{C65/68S}$, respectively, suggesting physical interaction between the two proteins (**Fig. 4g**). To determine whether March5 is the primary E3 enzyme that ubiquitinates and thus destabilizes Noxa, we assessed ubiquitinated Noxa levels in cells lacking either *March5*, *Ube2j2* or *Ube2k* via a tandem-

repeated ubiquitin-binding entities (TUBE) assay [33]. As expected, in the presence of MG132, protein bands representing polyubiquitinated Noxa were evident in WT mMA9Cas cells (**Fig. 4h**) but barely detectable in comparably treated *March5* KO cells, indicating that March5 is indeed the primary E3 that ubiquitinates Noxa. Similarly, ubiquitinated Noxa levels were significantly reduced in cells lacking either *Ube2j2* or *Ube2k* (**Fig. 4h**).

The Noxa-March5 axis regulates AML sensitivity to VEN by modulating Bax saturation of Bcl2, Bcl-XL and Mcl1

To define molecular mechanisms used by the March5-Noxa axis to regulate VEN and A-1155463 sensitivity, we first assessed interactions between BH3 mimetics and their targets in cells using a cellular thermal shift assay (CETSA) [34], a method based on the principle of ligand-induced thermal stabilization of a target protein. We pre-treated mMA9Cas^{M5FK} cells with either dTAG^{V-}1 or negative control ligand and then treated them with either VEN or control DMSO vehicle. One hour later, we heated cell suspensions to indicated temperatures and monitored whether Bcl2 protein is protected against heat-induced denaturation by VEN. Similarly, engagement of A-1155463 with Bcl-XL was assessed via CETSA using *March5* KO mMA9Cas cells. Both Bcl2 and Bcl-XL were heat-protected by respective BH3 mimetics regardless of March5 status, indicating that March5 does not modulate engagement of BH3 mimetics with their targets (**Supplemental Fig. 4a**).

We next asked whether Bax release from Bcl2 upon VEN treatment was altered by March5 depletion. To do so, we pre-treated mMA9Cas^{M5FK} cells expressing Myc-

tagged Bcl2 with either dTAG^{V-1} or negative control ligand and then treated cells with various doses of VEN. We then performed IP using anti-Myc (Bcl2) antibody and assessed Bax/Bcl2 interaction. Bax was comparably loaded onto Bcl2, regardless of March5 status, and released from Bcl2 by VEN treatment (**Fig. 5a** and **Supplemental Fig. 4b**). We confirmed these results via reciprocal IP using an anti-Bax antibody (**Fig. 5b** and **Supplemental Fig. 4c**).

VEN-mediated Bax release from Bcl2 occurred in both March5 intact and depleted cells (**Fig. 5a, b**), but mitochondrial apoptosis occurred only in March5-depleted cells (**Fig. 3d**). Thus, we hypothesized that Bax released from Bcl2 upon VEN treatment may be entrapped by Bcl-XL and/or Mcl1 in March5 intact cells. To test this, we performed IP using anti-Mcl1 or -Bcl-XL antibody in the presence or absence of March5 and monitored Bax engagement with Bcl-XL or Mcl1. Noxa reportedly binds to Mcl1 but not to Bcl-XL [35], and we observed a significant increase in the amount of Mcl1-bound Noxa in March5-depleted cells (**Fig. 5c** and **Supplemental Fig. 4d**). Strikingly, the amount of Bax bound to Mcl1 upon VEN treatment was significantly greater in March5-intact cells, suggesting that Bax freed from Bcl2 by VEN treatment is entrapped by Mcl1 (**Fig. 5c**). Furthermore, we observed significantly less Mcl1-bound Bax in March5-depleted cells regardless of VEN treatment, suggesting that Noxa, which is induced upon March5 depletion, binds to Mcl1 and potentially blocks interaction with Bax (**Fig. 5c**). Levels of Bcl-XL-bound Bax also increased upon VEN treatment, regardless of March5 status (**Fig. 5c**).

Collectively, our model suggests that Bax released from Bcl2 by VEN treatment may be entrapped by Mcl1 and/or Bcl-XL in March5-intact cells, while in March5-

depleted cells, Bax freed by VEN treatment is likely captured only by Bcl-XL, as Mcl1 BH3-binding grooves may be saturated by Noxa, allowing Bax to self-assemble at the MOM and thereby inducing mitochondrial apoptosis (**Fig. 5d**). Of note, *March5* deletion drastically enhanced sensitivity to Navitoclax (NAV), a Bcl2 and Bcl-XL dual inhibitor (**Supplemental Fig. 4e**), suggesting that Bax freed from Bcl2 and Bcl-XL by NAV treatment is not entrapped by any of the three anti-apoptotic proteins. Mechanistically, in that scenario, BH3-binding grooves of Bcl2 and Bcl-XL would likely be occupied by Navitoclax, while those of Mcl1 may be saturated by Noxa.

Discussion

VEN is becoming an important drug for AML therapy, particularly for patients ineligible for IC. When combined with Aza or LD-AraC, VEN treatment results in clinical outcomes superior to either Aza or LD-AraC alone [8,10]. Furthermore, IC plus VEN might also be a therapeutic option for AML patients eligible for IC [36]. In fact, a series of clinical trials combining VEN with chemotherapeutic- and/or molecularly-targeted drugs against hematologic malignancies is underway. [9,37,38]; however, molecular mechanisms underlying VEN sensitivity remain largely unknown. Here, we show that BAX saturation of Bcl2, Bcl-XL and Mcl1 is a key determinant of AML sensitivity to VEN and that targeting a mitochondrial E3 ligase complex comprised of MARCH5/UBE2J2/UBE2k could represent a novel means to overcome VEN resistance.

There have been few reports of biomarkers useful to predict VEN sensitivity or resistance. A positive association of *IDH1/2* mutations with VEN sensitivity was initially reported by the Majeti group based on a large-scale RNA interference screen [5]. These findings were later confirmed by real-world data indicating that patients harboring *IDH1/2* mutations respond well to VEN monotherapy and/or VEN plus Aza or LD-AraC combination therapies [6,8]. Other factors relevant to VEN resistance have also been reported [21,39-42]. Enhanced expression of MCL1[41], which is often observed in monocytic AML cells, BCL-XL [39] and/or BCL2A1 [43,44] reportedly confers resistance to VEN-induced apoptosis. Mutations within the BCL2 BH3-binding groove are associated with VEN resistance in chronic lymphocytic leukemia (CLL) [40]. *BAX* mutations, which impair the ability of BAX protein to localize properly to the MOM, are found in VEN-refractory CLL cases [42]. Mutations of *TP53* and/or RAS pathway genes are also implicated in VEN

304 resistance [39,44,45]. *PMAIP1* downregulation is reportedly associated with VEN resistance
305 in AML lines [39], but, to our knowledge, *PMAIP1* loss-of-function mutations have not
306 been reported in human AML cases. These biomarkers of VEN resistance are
307 particularly relevant to patients scheduled for VEN treatment, as that information could
308 guide physicians to alternate therapies. Since VEN is becoming a key component of
309 frontline AML therapy, it is also necessary to stratify patients “upfront” based on
310 biomarkers that predict VEN sensitivity. BH3 profiling [16] is a functional test that has
311 been proven useful as such a predictive biomarker; however, it is not generally available
312 in practice.

313 Improving treatment approaches for AML patients requires two differing but
314 complementary strategies. On the one hand, it is important to identify patients who
315 respond well to VEN based on predictive biomarkers. But on the other, it is also
316 important to develop interventions to broadly sensitize AML cells to VEN. Combining
317 BH3 mimetics, which target different anti-apoptotic proteins, with VEN treatment is a
318 reasonable approach to maximally induce mitochondrial apoptosis in leukemia cells. In
319 fact, VEN combined with low-dose NAV plus chemotherapy has shown promising
320 efficacy against relapsed/refractory acute lymphoblastic leukemia (ALL) [37]. However,
321 considering that BCL2/MCL1 expression levels vary among AML samples [13,39] and that
322 Mcl1 is essential for maintenance of mouse AML in vivo [46], targeting MCL1 either
323 directly or indirectly may be necessary to effectively induce mitochondrial apoptosis of
324 AML cells. In fact, combinatorial use of VEN and a MCL1 inhibitor has been proven
325 effective in pre-clinical AML models [47]; however, it remains unclear what the therapeutic
326 window is for MCL1 inhibitors due to potential on-target toxicities [4,9].

Targeting the March5 E3 ubiquitin complex mirrors Mcl1 inhibition via an MCL1 inhibitor to some extent, as it stabilizes Noxa protein, which may in turn saturate Mcl1 BH3-binding grooves (**Fig. 5d**). March5 depletion alone did not induce mitochondrial apoptosis of AML cells (**Fig. 3c, d**), in agreement with a report that overexpressed Noxa protein displaces Bak from Mcl1 and induces apoptosis only in *Bcl-XL*-KO, but not WT, mouse embryonic fibroblasts (MEFs) [35]. We conclude that Bax is the primary executor of VEN-induced mitochondrial apoptosis in *March5*-deficient AML cells, given that 1) VEN induces apoptosis in *Bak1/March5* DKO but not *Bax/March5* DKO cells (**Supplemental Fig. 2a**) and 2) sgRNAs targeting *Bax* were significantly enriched upon VEN treatment in our CRISPR screen of *March5* KO cells (**Fig. 4b** and **Supplemental Fig. 3a**).

In recent years multiple studies have suggested functional interactions between MARCH5 and the MCL1/NOXA complex [30-32,48]. However, here we show for the first time that in AML cells, March5, functioning primarily with Ube2j2/Ube2k E2-conjugating enzymes, directly binds Noxa, ubiquitinates it and promotes its degradation. It is noteworthy that: 1) depletion of either *Ube2j2* or *Ube2k* significantly increased Noxa protein levels (**Fig. 4c** and **4h**); 2) neither *Ube2j2* nor *Ube2k* was synthetic lethal to VEN in *March5* KO cells (**Fig. 4b**) and 3) ubiquitinated Noxa levels decreased in both single KO lines (**Fig. 4h**). Therefore, we propose that both Ube2j2 and Ube2k play major roles in March5-mediated Noxa ubiquitination/degradation. Our data also suggest functional redundancy of Ube2j2 and Ube2k, as Noxa protein levels were higher in *Ube2j2/Ube2k* DKO cells than in either single KO line (**Supplemental Fig. 3b**). Interestingly, in an in vitro binding assay, March5/Ube2j2 interaction was detectable, while March5/Ube2k

interaction was not (**Supplemental Fig. 1l**). Reasons for this outcome are currently unclear, although detection of March5/Ube2k interaction via conventional binding assays may be challenging due in part to their membranous localization.

While MARCH5 reportedly mediates MCL1 protein degradation [30-32], in our study Mcl1 protein levels were largely unaffected by March5 depletion (**Fig. 4h, Supplemental Figs. 3f** and **4d**). This observation suggests that E3s other than March5 regulate Mcl1 protein levels Noxa-dependently. Although the basis for these discrepant findings is unclear, mechanisms underlying MCL1 protein degradation may vary depending on cell type and/or variations in NOXA protein levels.

Our results suggest that pharmacological inhibition of activity of the March5/UBE2J2/UBE2K ubiquitin complex combined with VEN or NAV treatment could be a promising means to efficiently target multiple anti-apoptotic proteins in AML cells (**Fig. 5d**). Inhibition of the March5 E3 complex in combination with VEN plus Aza might also be an effective strategy, as Aza reportedly upregulates *PMAIP1* mRNA levels [49,50]. Thus, combining MARCH5 depletion with Aza treatment could boost NOXA levels via both transcriptional and post-translational mechanisms.

While we were preparing this manuscript, Stegmaier's group reported that MARCH5 depletion sensitizes human AML lines to VEN treatment [51]. They showed that NOXA protein levels increase upon MARCH5 depletion, but that such changes in NOXA levels did not necessarily account for cell death seen following MARCH5 depletion [51]. In contrast, our data indicate that NOXA is the key effector of mitochondrial apoptosis induced by March5 depletion. sgRNAs targeting *Pmaip1* were among the most significantly enriched in our genome-wide CRISPR/Cas9 screen in *March5* KO AML

cells (**Fig. 4b** and **Supplemental Fig. 3a**). We further validated these findings via dose-response curves: *Pmaip1* depletion significantly decreased sensitivity to VEN and A-1155463 observed upon March5 depletion (**Fig. 4e** and **Supplemental Fig. 3g**). Furthermore, *Pmaip1*/*March5* DKO AML cells failed to undergo mitochondrial apoptosis upon VEN or A-1155463 treatment (**Fig. 4f**). Our results collectively indicate that increased Noxa protein levels primarily account for enhanced VEN and A-1155463 sensitivity seen in *March5*-depleted AML cells. Since MARCH5 (a.k.a. MITOL [26]) is implicated in multiple aspects of mitochondrial biogenesis [52], including mitochondrial fusion or mitochondria/endoplasmic reticulum interaction, MARCH5 depletion could induce cell death independently of the mitochondrial apoptosis pathway, as described [20-22]. Of note, *Pmaip1/March5* DKO AML cells exhibited slightly enhanced sensitivity to VEN or A-1155463 relative to either *Pmaip1* single KO or WT cells (**Fig. 4e**), which may account for Noxa-independent cell death mechanisms [51].

In summary, we identified a mitochondrial E3 ubiquitin ligase complex comprised of MARCH5/UBE2J2/UBE2K as a key regulator of VEN sensitivity in AML cells. Our findings suggest that targeting the MARCH5 E3 ligase complex in combination with Venetoclax and/or Navitoclax could be a novel means to broadly sensitize AML cells to mitochondrial apoptosis.

Methods

CRISPR screens in mMA9Cas cells

The GeCKO v2 mouse library (purchased from Addgene) consists of two half-libraries (A and B), containing altogether 130,209 sgRNAs (67,405 in Library A and 62,804 in Library B) targeting 20,611 protein-coding genes and 1,175 miRNAs plus 1,000 non-targeting control sgRNAs. The plasmid pool was prepared as described (https://www.addgene.org/pooled-library/zhang-human-gecko-v2/). Library representation was validated via Miseq (Illumina), and genome-wide screens were performed as described [18,53]. Briefly, $1.2x10^8$ mMA9Cas cells were transduced at a transduction efficiency of 30% with the viral pool to achieve an average coverage of more than x500. Cells were treated with puromycin (Sigma) 24h after transduction (on day 1), and $1x10^7$ cells were harvested two days later (on day 3) to obtain input DNA. Cells were maintained 7 days without BH3 mimetics and then divided into DMSO vehicle-, Venetoclax- or S63845-treated groups and incubated 7 more days. Cells were then harvested and genomic DNA extracted to assess sgRNA representation.

Library preparation for next generation sequencing

Library preparation was performed as described [54]. sgRNA inserts were PCR-amplified from 130 ug genomic DNA using Herculase 2 fusion DNA polymerase (Agilent). Resulting PCR products were purified and sequenced on a NextSeq500 sequencer (Illumina) to assess change in abundance of each sgRNA between initial and final cell populations.

Acknowledgements

We thank the members of the Department of Medicine and Biosystemic Science and the Division of Precision Medicine at Kyushu University for assistance and helpful discussion, and Elise Lamar for critical reading of the manuscript. This work is supported in part by a Grant-in-Aid for Young Scientists (18K16089)(to Y.S.), a Grant-in-Aid for Young Scientists (19K17859), a Research Grant from the KANAE Foundation, the MSD Life Science Foundation, the Yasuda Medical Foundation, the Mochida Memorial Foundation for Medical and Pharmaceutical Research, the Shinnihon Foundation of Advanced Medical Treatment Research, the Takeda Science Foundation (to T.Y.), a Grant-in-Aid for Scientific Research (C)(21K08429), the Shinnihon Foundation of Advanced Medical Treatment Research, the Takeda Science Foundation (to K.M.), a Grant-in-Aid for Scientific Research (B)(22494899)(to Y.K.), a Grant-in-Aid for Scientific Research (C)(19K05544)(to T. Masuda), a Grant-in-Aid for Scientific Research (S)(16H06391)(to K.A.), a Grant-in-Aid for Scientific Research (A) (17H01567, 20H00540), an AMED under grant number 18063889 and a Grant-in-Aid for Scientific Research (S)(20H05699)(to T. Maeda).

Contribution

F.N., Y.S., T.Y. and T. Maeda designed CRISPR-Cas9 screen experiments. F.N., Y.S., T.Y., J.N., K.A. and T. Maeda reviewed CRISPR screen data. F.N., K.S., Y.S., T.Y., H.I., T.T., M.M., S.H., K.M., Y.K., and T. Masuda. executed CRISPR-Cas9 experiments and cell biology and molecular biology experiments. Y.S. and J.N. analyzed CRISPR screen data. F.N. and T. Maeda wrote the manuscript with help from all authors.

Conflict-of-interest disclosure

The authors declare no competing interests.

Correspondence

Takahiro Maeda, Division of Precision Medicine, Kyushu University Graduate School of Medical Sciences, 3-1-1 Maidashi, Higashi-ku, Fukuoka, Japan, 812-8582; e-mail: maeda.takahiro.294@m.kyushu-u.ac.jp

References

1 Papaemmanuil, E. *et al.* Genomic Classification and Prognosis in Acute Myeloid Leukemia. *N Engl J Med* **374**, 2209-2221 (2016). https://doi.org:10.1056/NEJMoa1516192

2 Short, N. J., Rytting, M. E. & Cortes, J. E. Acute myeloid leukaemia. *The Lancet* **392**, 593-606 (2018). https://doi.org:10.1016/s0140-6736(18)31041-9

3 Dohner, H. *et al.* Diagnosis and Management of AML in Adults: 2022 ELN Recommendations from an International Expert Panel. *Blood* (2022). https://doi.org:10.1182/blood.2022016867

4 Dohner, H., Wei, A. H. & Lowenberg, B. Towards precision medicine for AML. *Nat Rev Clin Oncol* (2021). https://doi.org:10.1038/s41571-021-00509-w

5 Chan, S. M. *et al.* Isocitrate dehydrogenase 1 and 2 mutations induce BCL-2 dependence in acute myeloid leukemia. *Nat Med* **21**, 178-184 (2015). https://doi.org:10.1038/nm.3788

6 Konopleva, M. *et al.* Efficacy and Biological Correlates of Response in a Phase II Study of Venetoclax Monotherapy in Patients with Acute Myelogenous Leukemia. *Cancer Discov* **6**, 1106-1117 (2016). https://doi.org:10.1158/2159-8290.CD-16-0313

7 Pollyea, D. A. *et al.* Venetoclax with azacitidine disrupts energy metabolism and targets leukemia stem cells in patients with acute myeloid leukemia. *Nat Med* **24**, 1859-1866 (2018). https://doi.org:10.1038/s41591-018-0233-1

8 DiNardo, C. D. *et al.* Azacitidine and Venetoclax in Previously Untreated Acute Myeloid Leukemia. *N Engl J Med* **383**, 617-629 (2020). https://doi.org:10.1056/NEJMoa2012971

9 Roberts, A. W., Wei, A. H. & Huang, D. C. S. BCL2 and MCL1 inhibitors for hematologic malignancies. *Blood* **138**, 1120-1136 (2021). https://doi.org:10.1182/blood.2020006785

10 Wei, A. H. *et al.* Venetoclax plus LDAC for newly diagnosed AML ineligible for intensive chemotherapy: a phase 3 randomized placebo-controlled trial. *Blood* **135**, 2137-2145 (2020). https://doi.org:10.1182/blood.2020004856

11 Park, C. M. *et al.* Discovery of an orally bioavailable small molecule inhibitor of prosurvival B-cell lymphoma 2 proteins. *J Med Chem* **51**, 6902-6915 (2008). https://doi.org:10.1021/jm800669s

12 Souers, A. J. *et al.* ABT-199, a potent and selective BCL-2 inhibitor, achieves antitumor activity while sparing platelets. *Nat Med* **19**, 202-208 (2013). https://doi.org:10.1038/nm.3048

13 Pan, R. *et al.* Selective BCL-2 inhibition by ABT-199 causes on-target cell death in acute myeloid leukemia. *Cancer Discov* **4**, 362-375 (2014). https://doi.org:10.1158/2159-8290.CD-13-0609

14 Walensky, L. D. Targeting BAX to drug death directly. *Nat Chem Biol* **15**, 657-665 (2019). https://doi.org:10.1038/s41589-019-0306-6

15 Diepstraten, S. T. *et al.* The manipulation of apoptosis for cancer therapy using BH3-mimetic drugs. *Nat Rev Cancer* (2021). https://doi.org:10.1038/s41568-021-00407-4

16 Vo, T. T. *et al.* Relative mitochondrial priming of myeloblasts and normal HSCs determines chemotherapeutic success in AML. *Cell* **151**, 344-355 (2012). https://doi.org:10.1016/j.cell.2012.08.038
17 Kotschy, A. *et al.* The MCL1 inhibitor S63845 is tolerable and effective in diverse cancer models. *Nature* **538**, 477-482 (2016). https://doi.org:10.1038/nature19830
18 Yamauchi, T. *et al.* Genome-wide CRISPR-Cas9 Screen Identifies Leukemia-Specific Dependence on a Pre-mRNA Metabolic Pathway Regulated by DCPS. *Cancer Cell* **33**, 386-400 e385 (2018). https://doi.org:10.1016/j.ccell.2018.01.012
19 Li, W. *et al.* Quality control, modeling, and visualization of CRISPR screens with MAGeCK-VISPR. *Genome Biol* **16**, 281 (2015). https://doi.org:10.1186/s13059-015-0843-6
20 Guièze, R. *et al.* Mitochondrial Reprogramming Underlies Resistance to BCL-2 Inhibition in Lymphoid Malignancies. *Cancer Cell* (2019). https://doi.org:10.1016/j.ccell.2019.08.005
21 Chen, X. *et al.* Targeting Mitochondrial Structure Sensitizes Acute Myeloid Leukemia to Venetoclax Treatment. *Cancer Discov* **9**, 890-909 (2019). https://doi.org:10.1158/2159-8290.CD-19-0117
22 Roca-Portoles, A. *et al.* Venetoclax causes metabolic reprogramming independent of BCL-2 inhibition. *Cell Death Dis* **11**, 616 (2020). https://doi.org:10.1038/s41419-020-02867-2
23 Wang, X. *et al.* Ube2j2 ubiquitinates hydroxylated amino acids on ER-associated degradation substrates. *J Cell Biol* **187**, 655-668 (2009). https://doi.org:10.1083/jcb.200908036
24 Middleton, A. J. & Day, C. L. The molecular basis of lysine 48 ubiquitin chain synthesis by Ube2K. *Sci Rep* **5**, 16793 (2015). https://doi.org:10.1038/srep16793
25 Zheng, N. & Shabek, N. Ubiquitin Ligases: Structure, Function, and Regulation. *Annu Rev Biochem* **86**, 129-157 (2017). https://doi.org:10.1146/annurev-biochem-060815-014922
26 Yonashiro, R. *et al.* A novel mitochondrial ubiquitin ligase plays a critical role in mitochondrial dynamics. *EMBO J* **25**, 3618-3626 (2006). https://doi.org:10.1038/sj.emboj.7601249
27 Tao, Z. F. *et al.* Discovery of a Potent and Selective BCL-XL Inhibitor with in Vivo Activity. *ACS Med Chem Lett* **5**, 1088-1093 (2014). https://doi.org:10.1021/ml5001867
28 Nabet, B. *et al.* The dTAG system for immediate and target-specific protein degradation. *Nat Chem Biol* **14**, 431-441 (2018). https://doi.org:10.1038/s41589-018-0021-8
29 Nabet, B. *et al.* Rapid and direct control of target protein levels with VHL-recruiting dTAG molecules. *Nat Commun* **11**, 4687 (2020). https://doi.org:10.1038/s41467-020-18377-w
30 Haschka, M. D. *et al.* MARCH5-dependent degradation of MCL1/NOXA complexes defines susceptibility to antimitotic drug treatment. *Cell Death Differ* **27**, 2297-2312 (2020). https://doi.org:10.1038/s41418-020-0503-6
31 Djajawi, T. M. *et al.* MARCH5 requires MTCH2 to coordinate proteasomal turnover of the MCL1:NOXA complex. *Cell Death Differ* **27**, 2484-2499 (2020). https://doi.org:10.1038/s41418-020-0517-0

32 Arai, S. *et al.* MARCH5 mediates NOXA-dependent MCL1 degradation driven by kinase inhibitors and integrated stress response activation. *Elife* **9** (2020). https://doi.org:10.7554/eLife.54954

33 Hjerpe, R. *et al.* Efficient protection and isolation of ubiquitylated proteins using tandem ubiquitin-binding entities. *EMBO Rep* **10**, 1250-1258 (2009). https://doi.org:10.1038/embor.2009.192

34 Martinez Molina, D. *et al.* Monitoring drug target engagement in cells and tissues using the cellular thermal shift assay. *Science* **341**, 84-87 (2013). https://doi.org:10.1126/science.1233606

35 Willis, S. N. *et al.* Proapoptotic Bak is sequestered by Mcl-1 and Bcl-xL, but not Bcl-2, until displaced by BH3-only proteins. *Genes Dev* **19**, 1294-1305 (2005). https://doi.org:10.1101/gad.1304105

36 Lachowiez, C. A. *et al.* Venetoclax combined with induction chemotherapy in patients with newly diagnosed acute myeloid leukaemia: a post-hoc, propensity score-matched, cohort study. *Lancet Haematol* **9**, e350-e360 (2022). https://doi.org:10.1016/S2352-3026(22)00076-X

37 Pullarkat, V. A. *et al.* Venetoclax and Navitoclax in Combination with Chemotherapy in Patients with Relapsed or Refractory Acute Lymphoblastic Leukemia and Lymphoblastic Lymphoma. *Cancer Discov* **11**, 1440-1453 (2021). https://doi.org:10.1158/2159-8290.CD-20-1465

38 Daver, N. *et al.* Venetoclax Plus Gilteritinib for FLT3-Mutated Relapsed/Refractory Acute Myeloid Leukemia. *J Clin Oncol*, JCO2200602 (2022). https://doi.org:10.1200/JCO.22.00602

39 Nechiporuk, T. *et al.* The TP53 Apoptotic Network Is a Primary Mediator of Resistance to BCL2 Inhibition in AML Cells. *Cancer Discov* **9**, 910-925 (2019). https://doi.org:10.1158/2159-8290.CD-19-0125

40 Blombery, P. *et al.* Acquisition of the Recurrent Gly101Val Mutation in BCL2 Confers Resistance to Venetoclax in Patients with Progressive Chronic Lymphocytic Leukemia. *Cancer Discov* **9**, 342-353 (2019). https://doi.org:10.1158/2159-8290.CD-18-1119

41 Pei, S. *et al.* Monocytic Subclones Confer Resistance to Venetoclax-Based Therapy in Acute Myeloid Leukemia Patients. *Cancer Discov* (2020). https://doi.org:10.1158/2159-8290.CD-19-0710

42 Blombery, P. *et al.* Clonal hematopoiesis, myeloid disorders and BAX-mutated myelopoiesis in patients receiving venetoclax for CLL. *Blood* (2021). https://doi.org:10.1182/blood.2021012775

43 Bisaillon, R. *et al.* Genetic characterization of ABT-199 sensitivity in human AML. *Leukemia* **34**, 63-74 (2020). https://doi.org:10.1038/s41375-019-0485-x

44 Zhang, H. *et al.* Integrated analysis of patient samples identifies biomarkers for venetoclax efficacy and combination strategies in acute myeloid leukemia. *Nat Cancer* **1**, 826-839 (2020). https://doi.org:10.1038/s43018-020-0103-x

45 DiNardo, C. D. *et al.* Molecular patterns of response and treatment failure after frontline venetoclax combinations in older patients with AML. *Blood* **135**, 791-803 (2020). https://doi.org:10.1182/blood.2019003988

46 Glaser, S. P. *et al.* Anti-apoptotic Mcl-1 is essential for the development and sustained growth of acute myeloid leukemia. *Genes Dev* **26**, 120-125 (2012). https://doi.org:10.1101/gad.182980.111

47 Thijssen, R. *et al.* Intact TP-53 function is essential for sustaining durable responses to BH3-mimetic drugs in leukemias. *Blood* **137**, 2721-2735 (2021). https://doi.org:10.1182/blood.2020010167

48 Subramanian, A., Andronache, A., Li, Y. C. & Wade, M. Inhibition of MARCH5 ubiquitin ligase abrogates MCL1-dependent resistance to BH3 mimetics via NOXA. *Oncotarget* **7**, 15986-16002 (2016). https://doi.org:10.18632/oncotarget.7558

49 Jin, S. *et al.* 5-Azacitidine Induces NOXA to Prime AML Cells for Venetoclax-Mediated Apoptosis. *Clin Cancer Res* **26**, 3371-3383 (2020). https://doi.org:10.1158/1078-0432.CCR-19-1900

50 Cojocari, D. *et al.* Pevonedistat and azacitidine upregulate NOXA (PMAIP1) to increase sensitivity to venetoclax in preclinical models of acute myeloid leukemia. *Haematologica* (2021). https://doi.org:10.3324/haematol.2020.272609

51 Lin, S. *et al.* An In Vivo CRISPR Screening Platform for Prioritizing Therapeutic Targets in AML. *Cancer Discov* **12**, 432-449 (2022). https://doi.org:10.1158/2159-8290.CD-20-1851

52 Nagashima, S., Tokuyama, T., Yonashiro, R., Inatome, R. & Yanagi, S. Roles of mitochondrial ubiquitin ligase MITOL/MARCH5 in mitochondrial dynamics and diseases. *J Biochem* **155**, 273-279 (2014). https://doi.org:10.1093/jb/mvu016

53 Sasaki, K. *et al.* Genome-wide CRISPR-Cas9 screen identifies rationally designed combination therapies for CRLF2-rearranged Ph-like ALL. *Blood* (2021). https://doi.org:10.1182/blood.2021012976

54 Shalem, O. *et al.* Genome-scale CRISPR-Cas9 knockout screening in human cells. *Science* **343**, 84-87 (2014). https://doi.org:10.1126/science.1247005

55 Colic, M. *et al.* Identifying chemogenetic interactions from CRISPR screens with drugZ. *Genome Med* **11**, 52 (2019). https://doi.org:10.1186/s13073-019-0665-3

56 Edlich, F. *et al.* Bcl-x(L) retrotranslocates Bax from the mitochondria into the cytosol. *Cell* **145**, 104-116 (2011). https://doi.org:10.1016/j.cell.2011.02.034

57 Schellenberg, B. *et al.* Bax exists in a dynamic equilibrium between the cytosol and mitochondria to control apoptotic priming. *Mol Cell* **49**, 959-971 (2013). https://doi.org:10.1016/j.molcel.2012.12.022

Figure legends

Fig. 1 A genome-wide CRISPR-Cas9 screen identifies components of the E3 ubiquitin ligase complex as key modulators of VEN sensitivity. a Schematic representation of the CRISPR-Cas9 screen. Mouse *MLL::AF9* AML cells stably expressing Cas9 (mMA9Cas) were transduced with the GeCKO library, selected in puromycin and cultured for 7 days, followed by 7 days of treatment with either DMSO, 3.5μM Venetoclax (BCL2 inhibitor) or 15μM S63845 (MCL1 inhibitor). **b** Dot graphs representing β-scores of 19,114 genes in the presence or absence of either Venetoclax (left) or S63845 (right). Genes whose β-scores exhibited statistically significant change upon drug treatment (FDR<0.1) are depicted in red. **c** Genes whose sgRNA abundance was significantly altered by VEN treatment were assessed using the DrugZ program[55]. Negative β scores represent genes essential for cell fitness. **d** mMA9Cas cells were transduced with a lentivirus vector encoding an sgRNA and Crimson cassette and cultured with or without VEN (5μM). Crimson-positive cell fractions were assayed by FACS at indicated times and proportions were normalized to the number of Crimson-positive cells present at day 0 (two days after transduction). Empty vector served as control. Each condition was assessed in triplicate, and data are represented as means ± SD. **e** Parental mMA9Cas cells (WT) and those deficient in either *Ube2j2*, *Ube2k* or *March5* were treated with VEN (5μM) and proportions of apoptotic cells were assessed by Annexin V stain 6h after treatment. Conditions were assessed in triplicate, and data are represented as means ± SD. P-values were calculated using one-way ANOVA. **f** Cleaved caspase 3 (C-casp3) levels, indicative of mitochondrial apoptosis, were assessed by Western blots. WT and mutant lines were treated with VEN at indicated doses, and protein lysates were obtained 6h after treatment. **g** mMA9Cas lines deficient

in either *Ube2j2, Ube2K* or *March5* were generated, and codon-optimized cDNA for each gene was added-back using lentiviral vectors that also express hKO1 protein. Cells were cultured with or without VEN (5μM), and proportions of hKO1-positive cells were assessed over 6 days by FACS.

Fig. 2 Ube2j2 and Ube2k function March5-dependently. a WT and *March5* KO mMA9Cas cells were transduced with a lentivirus vector encoding sgRNAs targeting either *Ube2j2* or *Ube2k* plus a Crimson cassette and then cultured with or without VEN (3μM). Crimson-positive cell fractions were measured at indicated times by FACS and normalized to the number of Crimson-positive cells present at day 0 (two days after transduction). Empty vector served as control. Conditions was assayed in triplicate, and data are represented as means ± SD. **b** *March5* KO mMA9Cas cells were transduced with either WT or ligase-mutant (H43W or C65/68S) March5 using lentiviral vectors also expressing humanized Kusabira Orange1 (hKO1). Proportions of hKO1-positive cells were assessed over 6 days by FACS, with or without VEN (3μM). Empty vector served as control. **c** Model showing interaction of the E2 ubiquitin-conjugating enzymes Ube2j2 and Ube2k with the E3 ligase March5 and a target substrate at the MOM.

Fig. 3 March5 depletion significantly sensitizes mMA9Cas cells to VEN or A-1155463 treatment. a WT and two *March5* KO lines (clones #1 and #2) were treated with either VEN, A-11563 or S63845 at indicated doses, and cell counts assessed 48h later. Counts at each dose were normalized to those of untreated controls. Each

condition was assessed in triplicate, and data are represented as means ± SD. **b** *March5* KO mMA9Cas cells stably expressing HA-FKBP12^{F36V}-tagged March5 (mMA9Cas^{M5FK}) were established. Cells were pre-treated 6h with either dTag^{V}-1 or negative control ligand (NEG) and then treated 48h with BH3 mimetics at indicated doses. Dose response curves were generated as described in (a). **c** mMA9Cas^{M5FK} cells were pre-treated 3h with either dTag^{V}-1 or negative control ligand and then with either VEN (10μM) or A-1155463 (0.1μM). Protein lysates were obtained at indicated time points, and cleaved caspase 3 (C-casp3) levels assessed by Western blot. **d** mMA9Cas^{M5FK} cells were treated with VEN or A-1155463 as described in (c). Protein lysates were obtained from cytosolic and mitochondrial fractions, and Bax and cytochrome c levels in each fraction were assessed by Western blots. **e** mMA9Cas^{M5FK} cells overexpressing either Bcl2, Bcl-XL or Mcl1 were established, and dose response curves generated as described in (a).

Fig. 4 A genome-wide CRIPSR screen in *March5* KO cells identifies Noxa as a March5 substrate relevant to VEN sensitivity. a Schematic representation of the CRISPR-Cas9 screen using *March5* KO mMA9Cas cells. **b** Shown are dot graphs representing β-scores in the presence (3μM) or absence of VEN. Genes whose β-scores exhibited a statistically significant change upon VEN treatment (FDR<0.05) are depicted in red. **c** Noxa protein levels in a series of mutant mMA9Cas lines, as assessed by Western blots. Expression levels of Bcl2, Bcl-XL and Mcl1 are also shown. Gapdh served as a loading control. **d** Noxa protein levels and their localization assessed by IF in mMA9Cas cells treated with either dTAG^{v}-1 or negative ligand. Cox4

686 served as a mitochondrial marker (left). Line scan plots show relative fluorescence
687 intensities of Noxa, Cox4, and DAPI within a defined area along corresponding arrow
688 shafts (right). **e** A series of mutant lines was treated 48h with either VEN or A-1155463
689 at various doses, and dose response curves generated as Figure 3A. **f** *Pmaip1*-WT or -
690 KO mMA9Cas^{M5FK} cells were pre-treated 3h with dTag^{V}-1 or negative control ligand
691 (NEG) and then with either VEN (10μM) or A-1155463 (0.1μM). Protein lysates were
692 obtained at indicated timepoints after VEN or A-1155463 treatment, and cleaved
693 caspase 3 levels were assessed by Western blots. **g** *March5* KO mMA9Cas cells stably
694 expressing Myc-tagged March5$^{C65/68S}$ mutant were generated, and interaction of
695 March5$^{C65/68S}$ with Noxa was assessed by immunoprecipitation (IP). IPs were performed
696 using anti-Myc (upper panel) or anti-Noxa (lower panel) antibodies, followed by Western
697 blots with anti-Noxa or -Myc antibody, respectively. **h** Levels of ubiquitinated Noxa, as
698 assessed by a tandem-repeated ubiquitin-binding entities (TUBE) assay, in the
699 presence or absence of MG132 (0.25μM).
700
701 **Fig. 5 The March5/Noxa axis regulates AML cells sensitivity to Venetoclax by**
702 **modulating BAX saturation of anti-apoptotic proteins. a** Bcl2/Bax interaction was
703 assessed by IP/Western blots. Specifically, mMA9Cas^{M5FK} cells expressing Myc-tagged
704 Bcl2 were generated. Cells were pre-treated 6h with either dTag^{V}-1 or negative control
705 ligand (NEG), followed by 3h of VEN treatment at indicated doses. IP was performed
706 using anti-Myc **a** or -Bax **b** antibodies, followed by Western blots with anti-Bax or -Myc
707 antibodies, respectively. **c** Interactions between antiapoptotic proteins (Mcl1 and Bcl-
708 XL) and Bax were assessed by IP/ Western blots. mMA9Cas^{M5FK} cells were pre-treated

709 1h with either dTag^{V}-1 or negative control ligand (NEG), followed by VEN treatment
710 (1.5h at 10μM). IP was performed using anti-Mcl1 (left panel) or -Bcl-XL (right panel)
711 antibody, followed by Western blots using antibodies against Bax, Noxa, Mcl1 and Bcl-
712 XL. **d** Proposed model for March5-mediated regulation of Bax saturation of antiapoptotic
713 proteins. Bax shuttles from the cytoplasm to the MOM, where it is held “in check” by
714 anti-apoptotic proteins [56,57]. Bax released from Bcl2 upon VEN treatment is entrapped
715 by Bcl-XL and Mcl1 in March5-intact cells, and thus cannot self-assemble and
716 permeabilize the MOM (left). By contrast, Noxa protein levels are upregulated by
717 March5 depletion, saturating Mcl1 BH3-binding grooves in March5-depleted cells. Thus,
718 Bax released from Bcl2 by VEN treatment is not captured by Mcl1, and significant levels
719 of Bax self-assemble at the MOM, inducing mitochondrial apoptosis (right). Green dots
720 represent cytochrome c**.**

Supplemental online material for

Targeting a mitochondrial E3 ubiquitin ligase complex to overcome AML cell-intrinsic Venetoclax resistance

Fumihiko Nakao, Kiyoko Setoguchi, Yuichiro Semba, Takuji Yamauchi, Jumpei Nogami, Kensuke Sasaki, Hiroshi Imanaga, Tatsuya Terasaki, Manaka Miyazaki, Shigeki Hirabayashi, Kohta Miyawaki, Yoshikane Kikushige, Takeshi Masuda, Koichi Akashi and Takahiro Maeda*

**To whom correspondence should be addressed.*

E-mail: maeda.takahiro.294@m.kyushu-u.ac.jp

This PDF file includes:

Supplemental Figure. 1

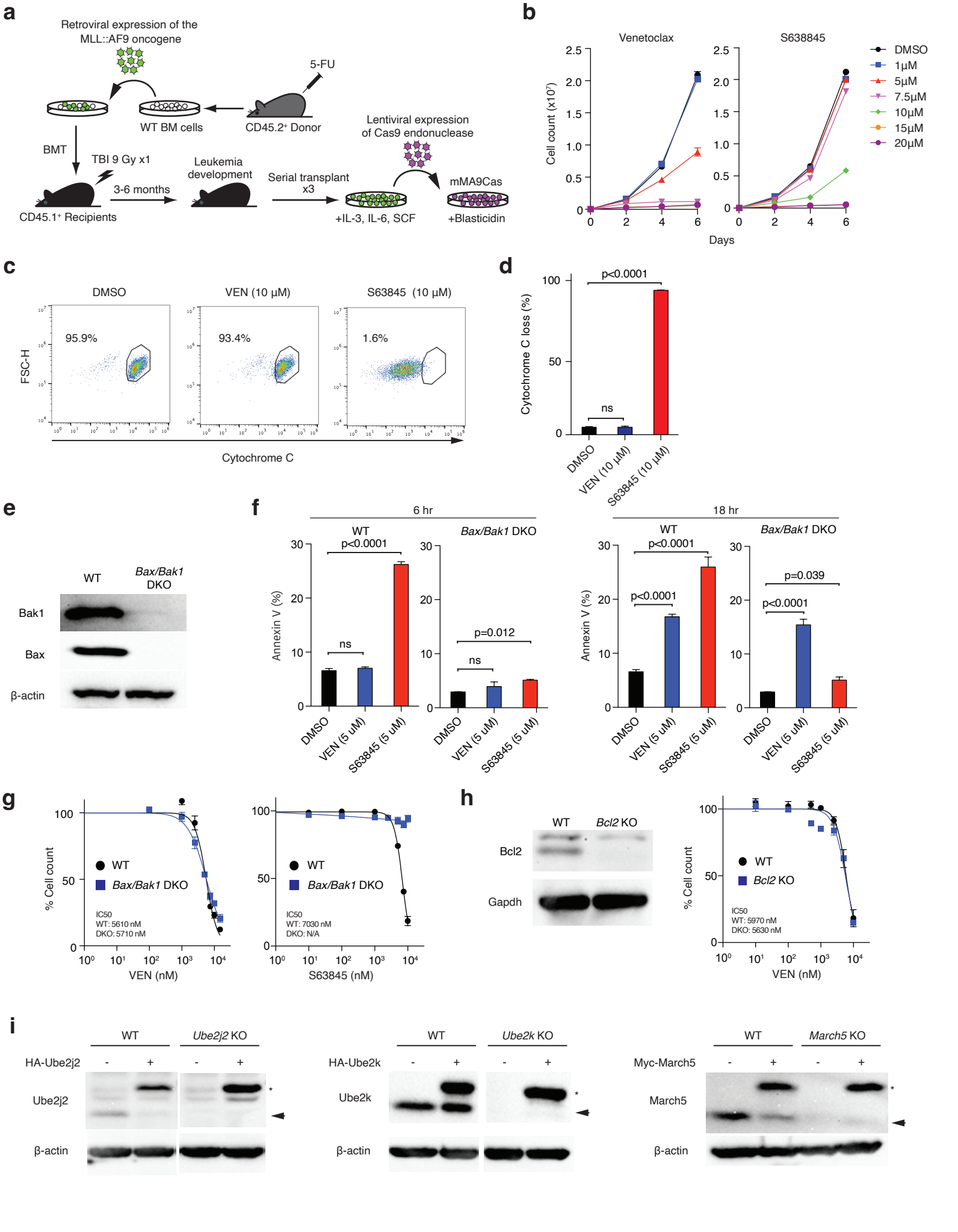

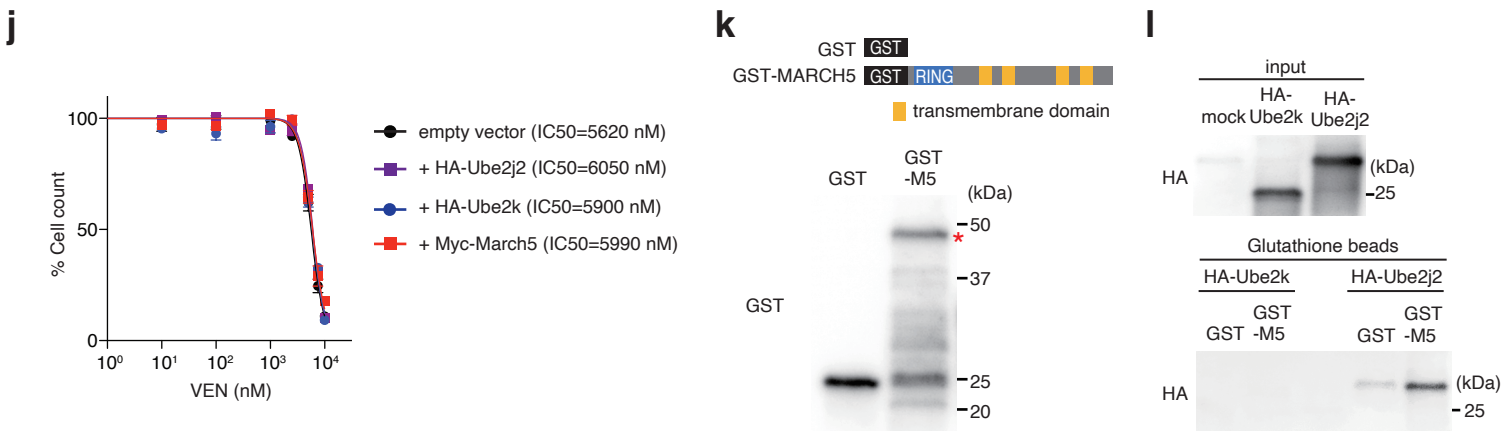

Supplemental Figure 1. Venetoclax fails to induce mitochondrial apoptosis in mMA9Cas cells. (a) Generation of mMA9Cas cells. CD45.2$^+$ bone marrow (BM) hematopoietic stem cells (HSCs) were retrovirally-transduced with the *MLL::AF9* fusion gene and transferred to lethally-irradiated recipients. After serial transplantation, AML cells were harvested and cultured in the presence of the cytokines and transduced with Cas9-expressing lentivirus to establish mMA9Cas cells [1]. **(b)** mMA9Cas cells were cultured 6 days in the presence of either VEN or S63845 at indicated doses, and growth curves were generated. **(c)** Cells were treated with either DMSO vehicle, VEN or S63845, and cytochrome c release from mitochondria was assessed by FACS 1h later. Representative FACS profiles are shown. **(d)** Bar graphs show proportions of cytochrome c released from mitochondria upon drug treatment. Each condition was assessed in triplicate, and data are represented as means ± SD. P-values were calculated using one-way ANOVA. **(e)** Western blots show Bak1 and Bax protein levels in WT and *Bax/Bak1* DKO mMA9Cas cells. **(f)** Proportions of apoptotic WT or *Bax/Bak1* DKO mMA9Cas cells, as assessed by Annexin V staining at 6h or 18h after treatment with indicated drugs. Each condition was examined in triplicate, and data are represented as means ± SD. P-values were calculated using one-way ANOVA. **(g)** WT and *Bax/Bak1* DKO mMA9Cas cells were treated with either VEN or S63845 at indicated doses, and cell counts were assessed 48h later. Cell counts at each dose were normalized to those of untreated controls. Each condition was assessed in triplicate, and data are represented as means ± SD. **(h)** Western blots showing absence of Bcl2 protein in *Bcl2* KO mMA9Cas cells (left). WT and *Bcl2* KO mMA9Cas cells were treated with VEN at indicated doses and counted 48h later. Counts at each dose were normalized to those of untreated controls. Each condition was assessed in triplicate, and data are represented as means ± SD (right). **(i)** Western blots show endogenous (arrowheads) and exogenous (asterisks) levels of indicated proteins. **(j)** mMA9Cas cells overexpressing either HA-Ube2j2, HA-Ube2k, Myc-March5 or empty vector were treated with VEN at indicated doses and counted 48h later. Counts at each dose were normalized to those of untreated controls. Each condition was assessed in triplicate, and data are represented as means ± SD. **(k)** Recombinant glutathione S-transferase (GST) and GST-tagged MARCH5 proteins were produced in E. coli cells and resolved by SDS-PAGE, followed by Western blotting with an anti-GST antibody. Asterisk denotes full-length GST-MARCH5 protein. **(l)** In vitro binding assays using recombinant GST-MARCH5 protein and protein lysates of HEK293FT cells overexpressing HA-tagged forms of either Ube2j2 or Ube2k. IPs were performed using GST beads, followed by Western blots with an anti-HA antibody.

Supplemental Figure. 2

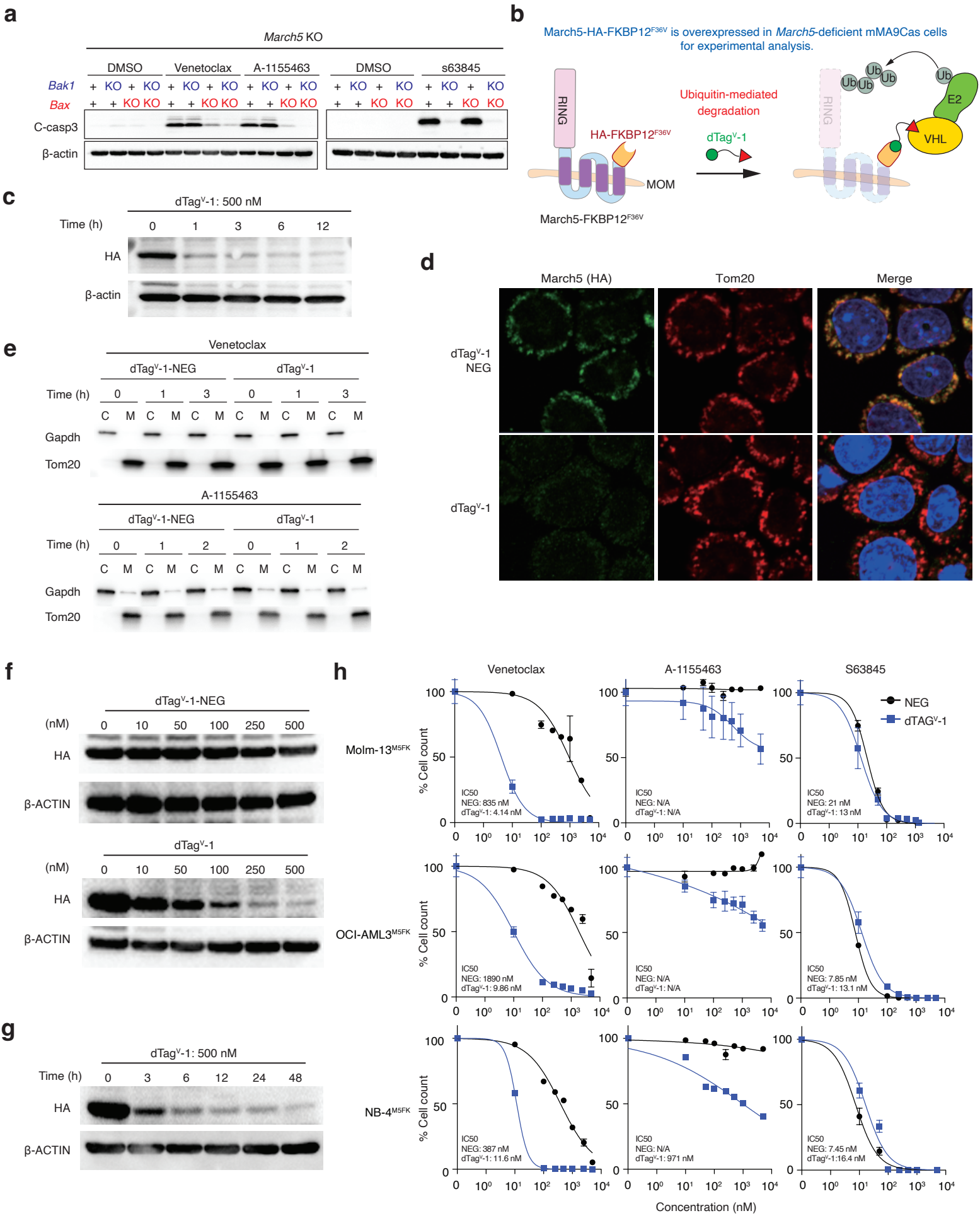

Supplemental Figure 2. MARCH5 depletion significantly enhances mouse or human AML cell sensitivity to VEN or A-1155463. (a) WT, *Bak1* KO, *Bax* KO and *Bak1/Bax* DKO AML cells were treated with either DMSO vehicle, VEN (5μM), A-1155463 (1μM) or s63845 (10μM) for 6h, and cleaved caspase 3 (C-casp3) levels were assessed by Western blot. **(b)** mMA9Cas^{M5FK} cells deficient in endogenous *March5* and overexpressing HA-FKBP12^{F36V}-tagged March5 were established. HA-FKBP12^{F36V}-tagged March5 protein was degraded via the ubiquitin/proteasome pathway upon dTag^{V}-1 ligand treatment. **(c)** HA-tagged March5 protein was degraded within 1-3h of dTag^{V}-1 ligand treatment. **(d)** dTag^{V}-1-mediated March5 depletion was confirmed by IF. Tom20, a mitochondrial import receptor subunit, served as a mitochondrial marker. **(e)** Fractionation of cytosolic (Gapdh) and mitochondrial (Tom20) proteins was validated by Western blots of protein lysates used in Figure 3d. **(f)** Human AML lines (Molm-13^{M5FK}, OCI-AML3^{M5FK} and NB-4^{M5FK}) were generated deficient in *MARCH5* and overexpressing HA-FKBP12^{F36V}-tagged MARCH5. HA-FKBP12^{F36V}-tagged MARCH5 protein was degraded upon dTag^{V}-1 ligand treatment in a dose **(f)**- and time **(g)**-dependent manner. Representative images of Molm-13^{M5FK} cells are shown. **(h)** Human AML lines deficient in endogenous *MARCH5* and overexpressing HA-FKBP12^{F36V}-tagged MARCH5 were pre-treated 6h with either dTag^{V}-1 or negative control (NEG) ligand and then treated 48h with either VEN, A-1155463 or S63845 at indicated doses. Cell counts at each dose were normalized to those of untreated controls, and dose response curves were generated. Each condition was assessed in triplicate, and data are represented as means ± SD.

Supplemental Figure. 3

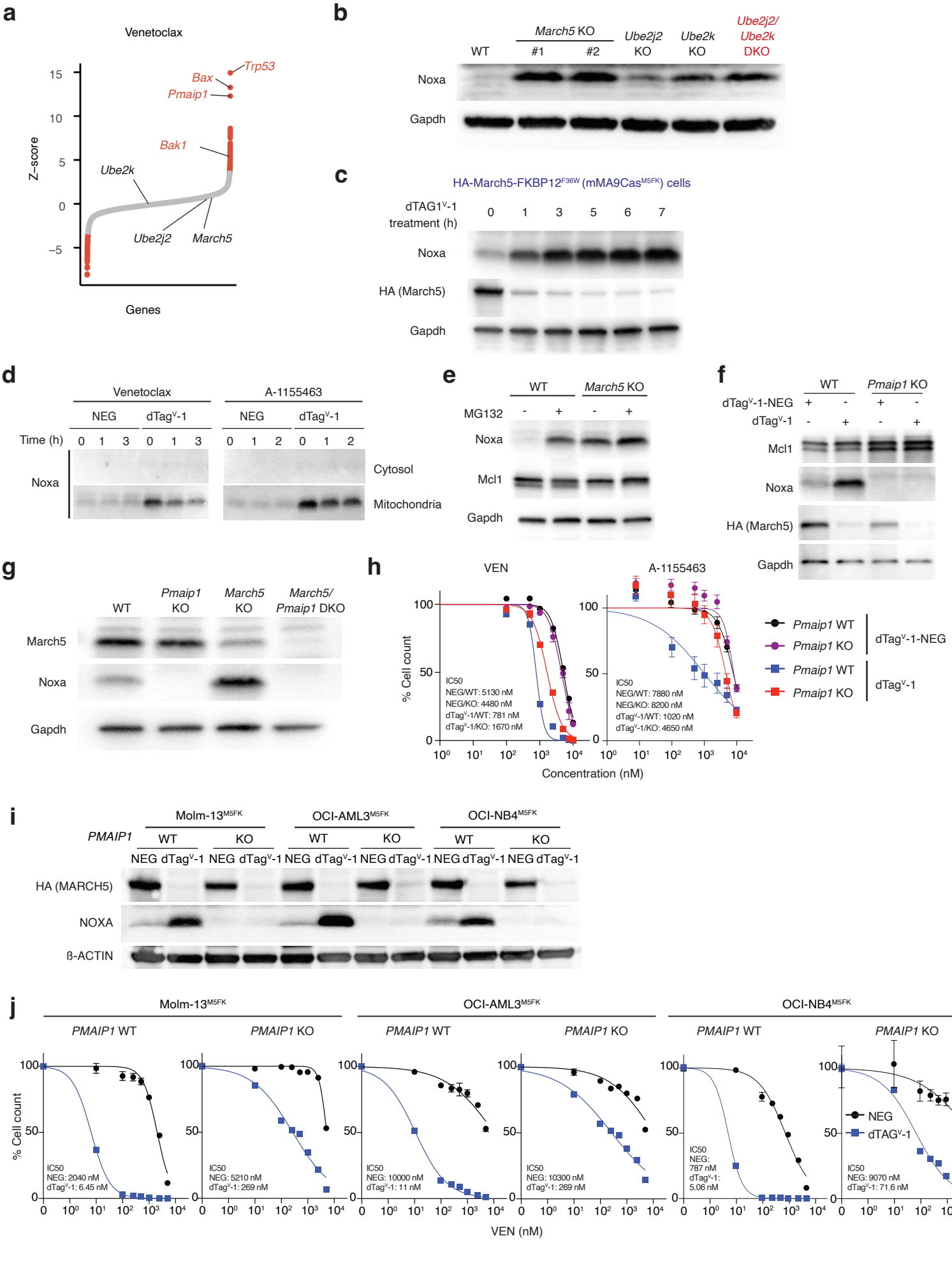

Supplemental Figure 3. *March5* depletion enhances AML cell sensitivity to VEN or A-1155463 Noxa-dependently. (a) Genes whose sgRNA abundance was significantly altered by VEN treatment were assessed using the DrugZ program [2]. Genes with positive or negative Z scores are plotted based on statistical significance. **(b)** Noxa protein levels in WT and mutant mMA9Cas cells were assessed by Western blot. Gapdh serves as a loading control. **(c)** Time course of changes in Noxa and March5 protein levels after $dTag^{V}$-1 treatment, based on Western blot analysis. **(d)** $mMA9Cas^{M5FK}$ cells were pre-treated 3h with either $dTag^{V}$-1 or negative control ligand (NEG) and then with either VEN or A-1155463. Protein lysates from cytosolic and mitochondrial fractions were obtained at indicated time points, and Western blots were performed. Noxa proteins were evident in the mitochondrial fraction. **(e)** Both WT and *March5* KO mMA9Cas cells were treated 4hr with MG132 (0.25μM), a proteasome inhibitor, prior to preparation of protein lysates. Noxa and Mcl1 protein levels were assessed by Western blots. Gapdh serves as a loading control. **(f)** *Pmaip1*-WT or -KO $mMA9Cas^{M5FK}$ cells were pre-treated 3h with either $dTag^{V}$-1 or negative control ligand (NEG) and subjected to Western blotting. Gapdh serves as a loading control. **(g)** March5 and Noxa protein levels in *March5/Pmaip1* DKO cells, as assessed by Western blotting. Gapdh serves as a loading control. **(h)** *Pmaip1*-WT or -KO $mMA9Cas^{M5FK}$ cells were pre-treated 6h with either $dTag^{V}$-1 or negative control ligand (NEG) and then with either VEN or A-1155463 for 48h at indicated doses. Cell counts at each dose were normalized to those of untreated controls, and dose response curves were generated. Each condition was assessed in triplicate, and data are represented as means ± SD. **(i)** Western blots show NOXA protein levels in *PMAIP1*-WT and -KO human AML lines ($Molm\text{-}13^{M5FK}$, $OCI\text{-}AML3^{M5FK}$ and $NB4^{M5FK}$) pretreated with $dTag^{V}$-1 or negative control ligand (NEG). **(j)** Dose response curves of indicated *PMAIP1*-WT or -KO human AML lines pre-treated 6h with either $dTag^{V}$-1 or NEG and then with VEN at indicated doses.

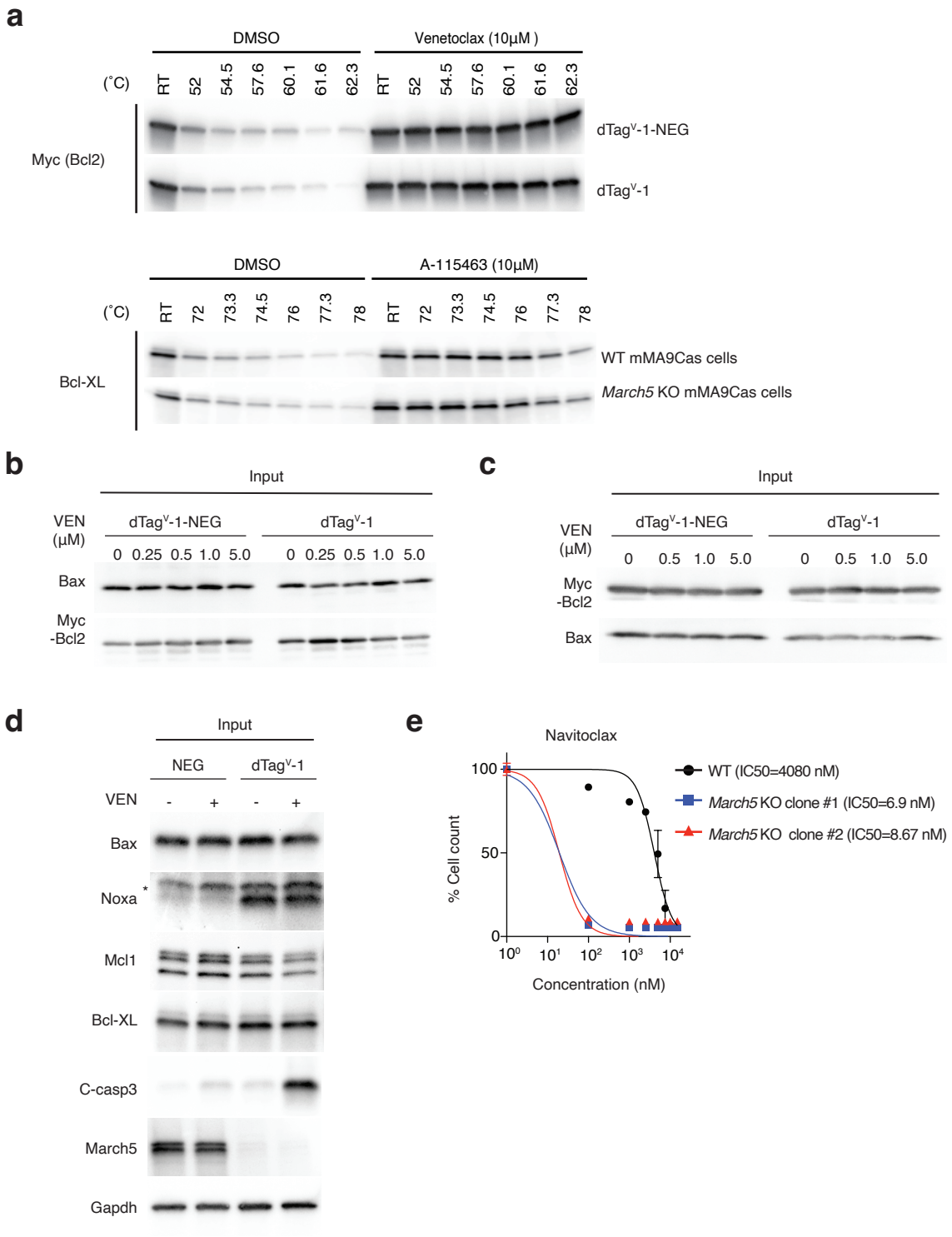

Supplemental Figure. 4 March5 regulates AML cell sensitivity to VEN by modulating Bax saturation of antiapoptotic proteins. a Representative data derived from cellular thermal shift assays (CETSA). To assess VEN/Bcl2 interaction, mMA9Cas^{M5FK} cells were pre-treated 3h with either dTag^{V}-1 or negative ligand (NEG) and then with either VEN (10μM) or DMSO vehicle for 1h. Protein lysates were obtained and heated to various temperatures. Soluble fractions of each lysate were collected and subjected to Western blotting. Engagement of A-1155463 with Bcl-XL was also assessed via CETSA using *March5* KO mMA9Cas cells. **b,c,d** Western blots were performed using 1% of protein lysates used for IP experiments (described in **Fig. 5a-c**). **e** WT and two *March5* KO lines were treated with Navitoclax at indicated doses, and cell counts were assessed 48h later. Cell counts at each dose were normalized to those of untreated control, and dose response curves were generated. Each condition was assessed in triplicate, and data are represented as means ± SD.

Supplemental Methods

Generation of Cas9-expressing AML lines

A mouse AML line expressing the *MLL::AF9* fusion and Cas9 (mMA9Cas) were previously described [1]. Human AML cells (Molm-13, OCI-AML3, NB-4) stably expressing Cas9 were established using lentivirus encoding both S. pyogenes Cas9 protein and the blasticidin resistance gene (lentiCas9-Blast, Addgene). Blastcidin selection was initiated 24hr after transduction.

CRISPR screen in *March5* KO mMA9Cas cells

The Brie library [purchased from Addgene (plasmid #73632)] includes 78,637 sgRNAs, namely, an average of 4 sgRNAs per gene, and 1000 non-targeting control sgRNAs. The plasmid pool was prepared as described (https://www.addgene.org/static/cms/filer_public/56/71/5671c68a-1463-4ec8-9db5-761fae99265d/broadgpp-pdna-library-amplification.pdf). The sgRNA library was transduced into $2.88x10^8$ *March5* KO mMA9Cas cells via lentivirus infection. Cells were treated with puromycin on day 1, and $2.2x10^7$ cells were harvested on day 3 to obtain input DNA. Cells were maintained 7 days without VEN and then divided into DMSO vehicle- or Venetoclax-treated groups and incubated 7 more days. Cells were then harvested, and genomic DNA extracted. Screens were performed in duplicate in each condition.

Cell culture

Mouse AML cells were cultured in Iscove's Modified Dulbecco's Media (IMDM) (Life Technologies) supplemented with 20% Fetal Bovine Serμ (FBS) (Omega Scientific), 1% penicillin streptomycin (Life Technologies), and mouse SCF (20 ng/ml), mouse IL-3 (10 ng/ml) and mouse IL-6 (10 ng/ml) (all from PeproTech). Human leukemia cell lines [MOLM-13 (JCRB cell bank), OCI-AML3 (DSMZ) and NB4 (DSMZ)] were cultured in Roswell Park Memorial Institute (RPMI) medium (FUJIFILM Wako Pure Chemical Corporation) with 10% FBS and 1% penicillin streptomycin. $dTAG^V$-1 and $dTAG^V$-1-NEG were purchased from Tocris Bioscience.

Lentiviral transduction

When 80% confluent, cells in 10mL media were transfected with packaging vectors [6.7 µg psPAX2 (Addgene) and 4.1 µg pMD2.G (Addgene), or 5.9 µg pCAG-HIVgp and 5.9 µg pCMV-VSV-G-RSV-REV (https://dna.brc.riken.jp/en/rvden/cfmen/cfm_plisten)] plus 10 µg lentiviral vectors using 60 µg of linear polyethylenimine (Polysciences). Medium was changed 8 hours after transfection. Lentiviral supernatants were harvested at 48- and 72-hours post-transfection and concentrated by ultracentrifugation (100,000 g for 2 hours at 4^{o}C with a HITACHI CS100FNX S50A-2254 rotor). AML cells were plated into 12-well plates (1-3 x 10^6 cells per well) with medium supplemented with 8 µg/ml polybrene (SantaCruz) and spin-infected at 2,000 rpm for 2 hours at 37^{o}C [1].

Immunoblotting

Cells were lysed with SDS buffer [40 mM Tris–HCl (pH 6.8), 3% glycerol, and 1% SDS]. Protein concentrations were measured using the BCA assay (Pierce). Lysates were resolved by SDS-PAGE and transferred to PVDF membranes, which were then immunoblotted with the following antibodies: Bax (Abcam, ab-32503), Bak1 [Cell signaling technologies (CST), #3814], Cytochrome c (BD bioscience, #556433), NOXA [Mouse: Prosci, #2437, Human: Abcam, ab-13654], Bcl2 (Santa Cruz,sc-7382), Mcl1 (CST, #5453), Bcl-XL (Santa Cruz, sc-8392), Myc (CST, #2276), HA (Abcam, ab-9110), March5 (Abcepta, AP5677a), Ube2j2 (Proteintech, 17713-1-AP), Ube2k (Abcam, ab-52930), Tom20 (Proteintech, 11802-1-AP), Actb (Sigma Aldrich, A-1978), Gapdh (CST, #5174).

Cell fractionation

Cytosol and organelle fractions were separated by centrifugation as described [3]. Briefly, 2x10^6 cells were washed once with wash buffer (20 mM Hepes-KOH, pH7.4, 0.25 M Sucrose, 25 mM KCL, and protease inhibitors) and then permeabilized 3 min with wash buffer containing 200 ug/mL Digitonin at 37^{o}C, followed by centrifugation at 20,000 g for 5 min.

MOMP assay

MOMP (Mitochondrial outer membrane permeabilization) was assessed by flowcytometry as described (http://letailab.dana-farber.org/uploads/6/8/9/2/68921131/bh3_ibh3.pdf). Briefly, $2.5x10^5$ cells were permeabilized with MEB buffer containing 20 µg/ml of digitonin, treated with indicated drugs, and incubated 30-45 min at 37°C. Cells were then fixed with 4% formaldehyde for 10 min and stained with anti-Cytochrome c antibody (Biolegend, #612310) overnight on ice, followed by FACS analysis.

Cell viability and apoptosis assays

Venetoclax, A-1155463 and S63845 were purchased from Chemietek. Cell viability was assessed using a Cell Counting Kit-8 (DOJINDO). Annexin V Binding Buffer (BD Biosciences) and APC-Annexin V antibody (BioLegend) were used to detect apoptotic cells by FACS. Cleaved caspase 3 levels were assessed by Western blots using Cleaved Casp3 antibody (CST, #9661).

Cell competition assay

AML cells were transduced with lentivirus vectors encoding sgRNAs and reporter proteins, such as Crimson and humanized Kusabira Orange1 (hKO1). Transduced cells were co-cultured with non-transduced cells and treated with indicated BH3 mimetics. Proportions of transduced cells were monitored over time by FACS.

Immunoprecipitation

$1x10^7$ cells were lysed with buffer containing 50 mM Tris-HCl (pH 7.5), 150 mM NaCl, 1% Triton X-100, 10% glycerol, and protease inhibitors, followed by centrifugation at 20,000g for 10 min. Immunoprecipitation was performed using the following antibodies: Bcl2 (CST, #3498), Mcl1 (CST, #94296), BclXL (CST, #2764), Myc (CST, #2276) and Bax (Abcam, ab-32503). Protein Dynabeads™

Protein G (Invitrogen) were used to isolate antibody/protein complexes, and immunoprecipitants were resolved by SDS-PAGE.

Immunofluorescence confocal microscopy

Cells were deposited onto a glass slide via Cytospin (Thermo Scientific), fixed for 15 min at room temperature with pre-warmed 4% PFA and then permeabilized with 1% Triton X-100 in PBS for 5 min, followed by incubation with primary antibodies. After incubation with Alexa Fluor-conjugated secondary antibodies (Invitrogen), images were acquired using a LSM 780 confocal microscope (Carl Zeiss). Relative fluorescence intensities of Noxa, Cox4, and DAPI within a defined area were assessed using ZEN software (Carl Zeiss, Inc.).

Cellular Thermal Shift Assay (CETSA)

CETSA was performed to assess engagement of BH3 mimetics with targets as described [4]. Briefly, $2x10^6$ cells were treated with either VEN or A-115463 for 1h, washed with PBS and resuspended in PBS. Cell suspensions were then heated to desired temperatures for 3 min and lysed with 1% NP40 for 20 min on ice. Soluble fractions were obtained by centrifugation at 20,000g, resolved by SDS-PAGE and subjected to Western blotting.

CRISPR/Cas9-mediated gene knockout

Two individual sgRNAs each targeting *Ube2j2*, *Ube2k*, *March5, Bax, Bak1, Pmaip1* (mouse) and *MARCH5* (human) were selected from the GeCKO v2 library or designed using an online tool (http://guides.sanjanalab.org/#/). sgRNAs were cloned into lentiGuide-Puro (Addgene) and/or lentiGuide-Crimson (Addgene) vectors. Lentivirus transduction was performed as described.

Recombinant protein production and in vitro binding assay

Human MARCH5 cDNA was subcloned into the pGEX-6P-2 vector (Cytiva). Glutathione S-transferase (GST)-fused MARCH5 protein were produced in E. coli BL21 (DE3) cells using a standard protocol. Briefly, E. coli cells were cultured overnight and then diluted to 1:10 (A600 = ~0.6). Protein expression was induced with isopropyl-β-D-thiogalactopyranoside (0.1mM) either at 37^{o}C for 2h or at 18^{o}C for 16h. Cells were then harvested, resuspended in ice-cold suspension buffer (50 mM Tris-HCl, pH 7.5, 150 mM NaCl, 10% glycerol, 1 mM phenylmethylsulfonyl fluoride, 1 mM EDTA), sonicated, and resuspended in 1% Triton X-100 solution. Protein lysates were collected after centrifugation at 16,000 g for 10min at 4^{o}C and then mixed with Glutathione Sepharose 4B beads (Cytiva). After 2h incubation with rotation at 4^{o}C, beads were washed with wash buffer (suspension buffer containing 1% Triton X-100) for three times. To quantitate the amount of purified GST or GST-tagged MARCH5 proteins, a small portion of beads was boiled with sample buffer, and eluted protein were resolved by SDS-PAGE, followed by Coomassie brilliant blue staining. GST-bound beads were mixed with cell lysates of HEK293FT cells overexpressing HA-tagged forms of either Ube2j2 or Ube2k and incubated with rotation for 2h at 4^{o}C. Beads were washed three times with wash buffer and then boiled with sample buffer. Resultant protein lysates were resolved by SDS-page and subjected to Western blotting.

Isolation of ubiquitinated proteins using tandem ubiquitin-binding entities (TUBEs)

1x10^{7} mMA9Cas cells were treated 4h with MG132 (0.25μM), spun-down, washed twice with ice-cold PBS and incubated with the TUBEs lysis buffer (20 mM HEPES-KOH, 150 mM NaCl, 10 % Glycerol, 1 % Triton X-100, 10 mM N-ethylmaleimide containing phosSTOP phosphatase inhibitors and cOmplete protease inhibitors, Roche) for 30 min on ice. Resultant protein lysates were incubated with the TUBEs-coupled agarose beads (LifeSensors) with rotation for 2h at 4^{o}C. Beads were then harvested, washed three times with wash buffer, and boiled with sample buffer. The eluates, which contain ubiquitinated proteins, were resolved by SDS page and subjected to Western blotting.

Plasmids

Plasmids used in this study were as follows: pMSCV-IRES-huCD2, pMSCV-mBCL2-huCD2, pMSCV-Mcl1-huCD2 (kind gifts from Dr. John Clohessy), CSII-EF-MCS-IRES2-hKO1 (RDB07915, RIKEN BRC), CSII-EF-MCS-IRES2-TagBFP, CSII-EF-MCS-HA-Ube2j2-hKO1, CSII-EF-MCS-HA-Ube2k-hKO1, CSII-EF-MCS-Myc-March5-hKO1, CSII-EF-MCS-Myc-March5_CSmut-hKO1, CSII-EF-MCS-Myc-March5_HWmut-hKO1, CSII-EF-MCS-HA-BclXL-TagBFP, Lenti_EFS_CdTag_PuroR, Lenti_EFS_CdTag_HA-MARCH5_PuroR, pHKO9-Crimson, pHKO9-PuroR (kind gifts from Dr. Dan Bauer), pHKO9-hKO1, pCAG-HIVgp (RDB04394, RIKEN BRC), pCMV-VSV-G-RSV-REV (RDB04393, RIKEN BRC), psPAX2 (Plasmid #12260, Addgene) and pMD2.G (Plasmid #12259, Addgene). For lentivirus-mediated gene knockouts, sgRNA-specifying oligos were subcloned into either lentiGuide-Puro (Addgene plasmid ID 52963) or lentiGuide-Crimson (Addgene plasmid ID 70683) vector. sgRNA sequences were as follows: *Ube2j2* #1: CCTGGGGAGCATAGAGACGT; *Ube2j2* #2: CCGACGTCTCTATGCTCCCC; *Ube2k* #1: CCTGTGACGGAACTAATATT; *Ube2k* #2: CCTAATATTAGTTCCGTCAC; *March5* #1: TGTCACTGCTCCATAAGTCA; *March5* #2: AAGTACTCGGCGTTGCACTG; *Bax* #1: CCAGTTCATCTCCAATTCGC; *Bax* #2: GCTTGTCTGGATCCAAGACC; *Bak1* #1: TCTTCACCAAGATCGCCTCC; *Bak1* #2: TGCATCATTACATCGCCAGA; *Bcl2* #1: CATCTGACCCTCCGCCGGGC; *Bcl2* #2: ACATCTCTGCGAAGTCACGA; *Pmaip1* #1: ACGCGCCAGTGAACCCAACG; *Pmaip1* #2: GCAGCTCAACTCAGGAAGAT; *MARCH5* #1: TGGGTGGATGAAAAGCAAAG; *MARCH5* #2: GGCCTGTCTACAACGCTGGG; *PMAIP1* #1: CGCTCAACCGAGCCCCGCGC; *PMAIP1* #2: TCGAGTGTGCTACTCAACTC. Details of the plasmids will be provided upon requests.

Supplemental References

1 Yamauchi, T. *et al.* Genome-wide CRISPR-Cas9 Screen Identifies Leukemia-Specific Dependence on a Pre-mRNA Metabolic Pathway Regulated by DCPS. *Cancer Cell* **33**, 386-400 e385 (2018). https://doi.org:10.1016/j.ccell.2018.01.012

2 Colic, M. *et al.* Identifying chemogenetic interactions from CRISPR screens with drugZ. *Genome Med* **11**, 52 (2019). https://doi.org:10.1186/s13073-019-0665-3

3 Mikhailov, V. *et al.* Bcl-2 prevents Bax oligomerization in the mitochondrial outer membrane. *J Biol Chem* **276**, 18361-18374 (2001). https://doi.org:10.1074/jbc.M100655200

4 Martinez Molina, D. *et al.* Monitoring drug target engagement in cells and tissues using the cellular thermal shift assay. *Science* **341**, 84-87 (2013). https://doi.org:10.1126/science.1233606

Fig. 1

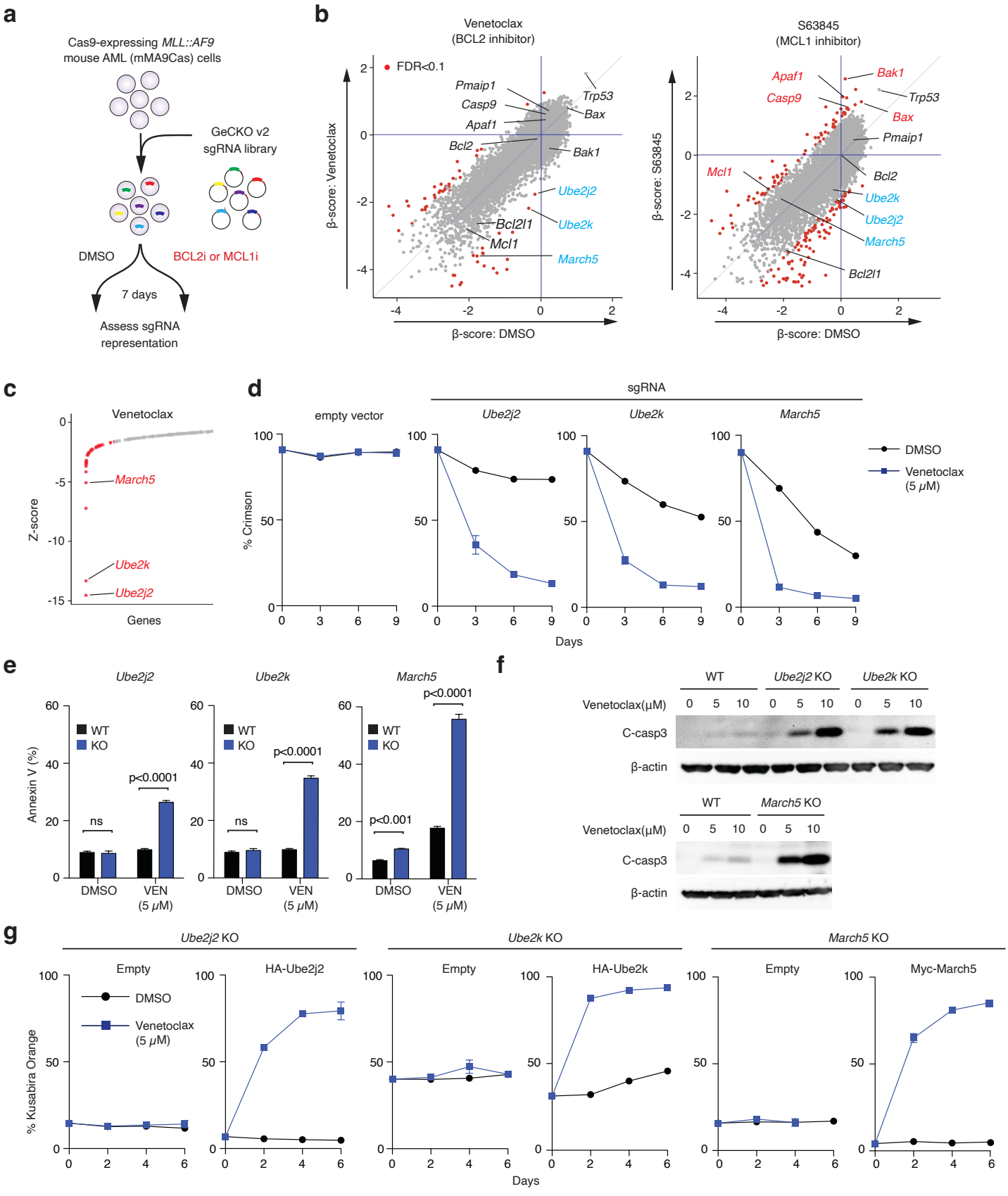
a
Cas9-expressing MLL::AF9
mouse AML (mMA9Cas) cells
GeCKO v2
sgRNA library
DMSO
BCL2i or MCL1i
7 days
Assess sgRNA
representation
b
Venetoclax
(BCL2 inhibitor)
S63845
(MCL1 inhibitor)
FDR<0.1
β-score: Venetoclax
β-score: S63845
β-score: DMSO
Pmaip1
Casp9
Apaf1
Bcl2
Trp53
Bax
Bak1
Ube2j2
Ube2k
Bcl2l1
Mcl1
March5
c
Venetoclax
Z-score
Genes
March5
Ube2k
Ube2j2
d
sgRNA
empty vector
Ube2j2
Ube2k
March5
% Crimson
Days
DMSO
Venetoclax
(5 μM)
e
Ube2j2
Ube2k
March5
Annexin V (%)
WT
KO
p<0.0001
p<0.001
ns
DMSO
VEN
(5 μM)
f
WT
Ube2j2 KO
Ube2k KO
March5 KO
Venetoclax(μM)
0 5 10
C-casp3
β-actin
g
Ube2j2 KO
Ube2k KO
March5 KO
Empty
HA-Ube2j2
HA-Ube2k
Myc-March5
% Kusabira Orange
DMSO
Venetoclax
(5 μM)
Days

Fig. 2

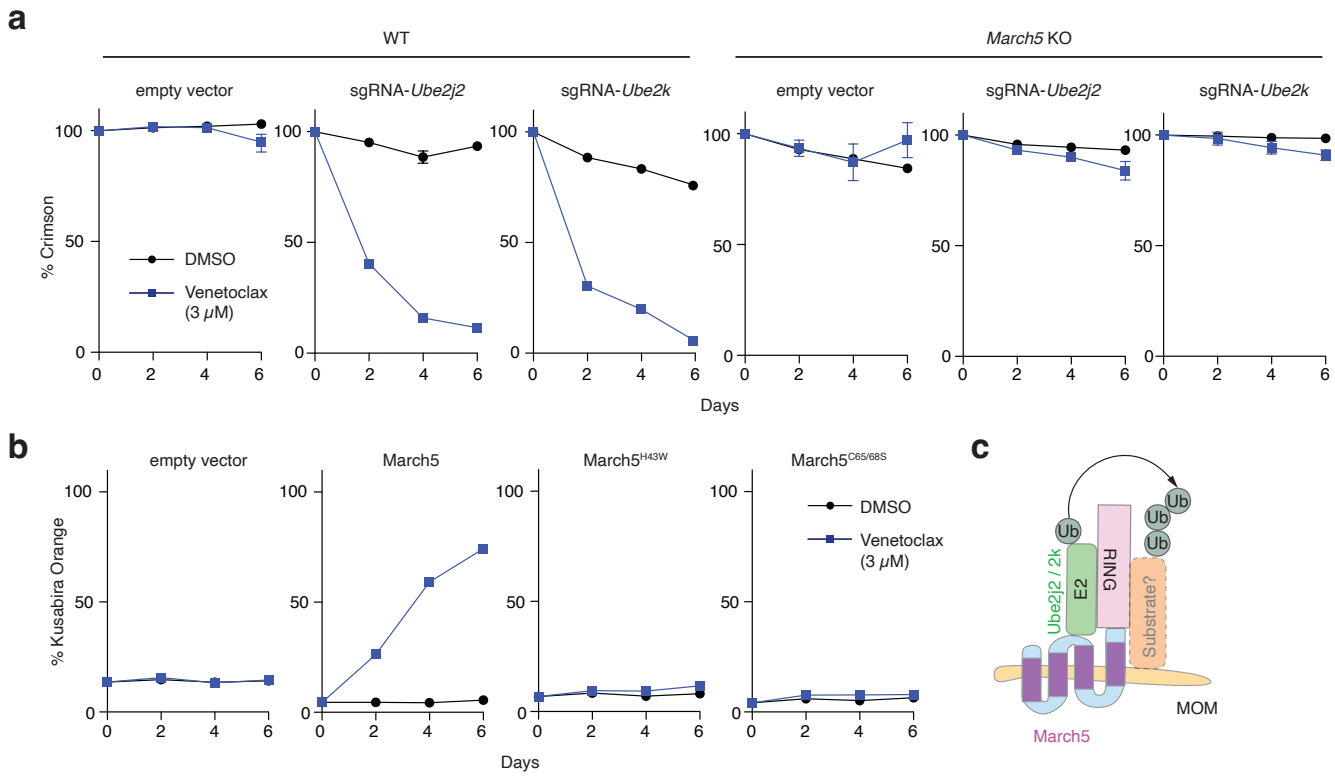
a
WT
March5 KO
empty vector
sgRNA-Ube2j2
sgRNA-Ube2k
empty vector
sgRNA-Ube2j2
sgRNA-Ube2k
% Crimson
DMSO
Venetoclax
(3 μM)
Days
b
empty vector
March5
March5H43W
March5C65/68S
% Kusabira Orange
DMSO
Venetoclax
(3 μM)
Days
c
Ub
Ub
Ub
Ub
Ube2j2 / 2k
E2
RING
Substrate?
MOM
March5

Fig. 3

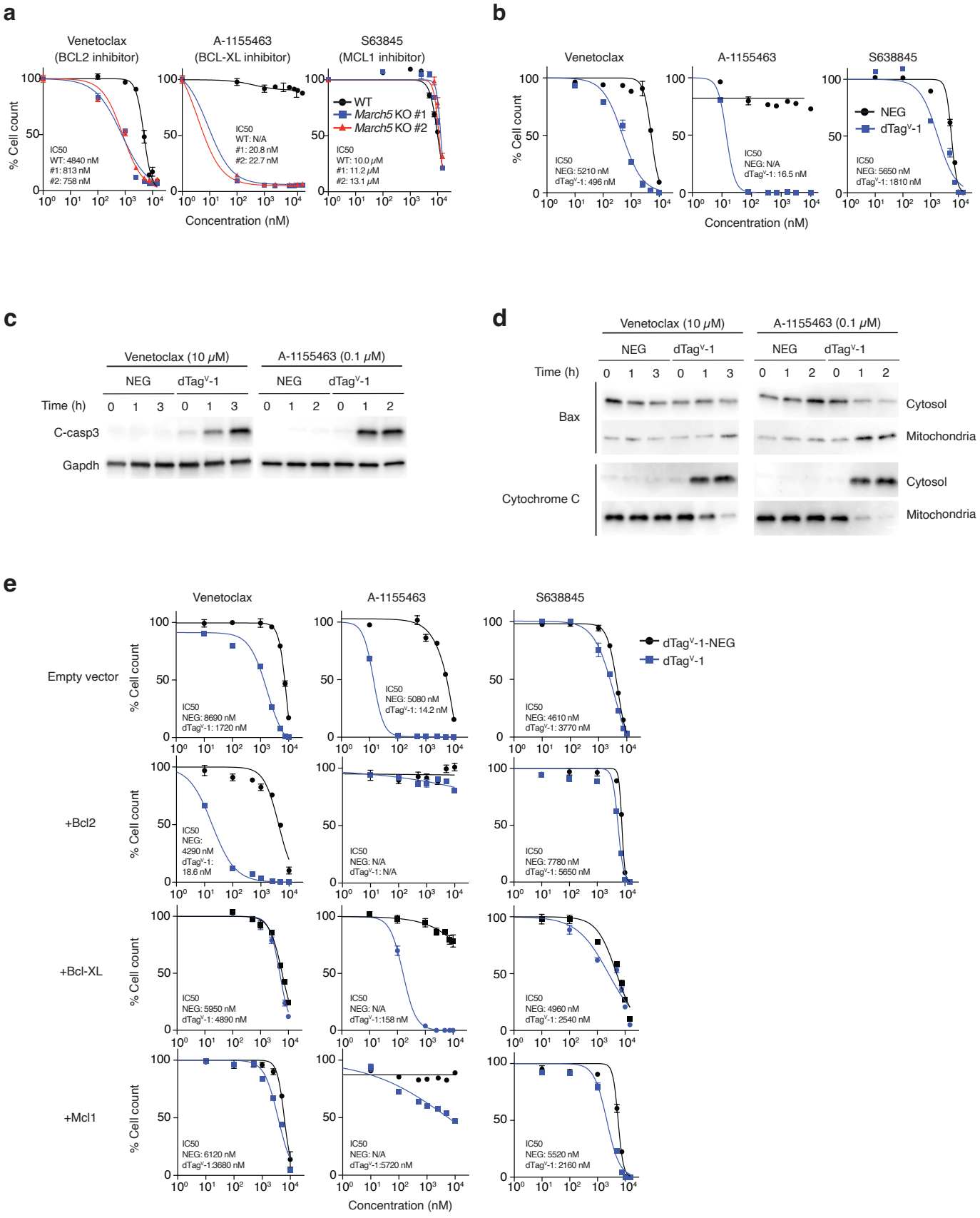
a
Venetoclax (BCL2 inhibitor)
A-1155463 (BCL-XL inhibitor)
S63845 (MCL1 inhibitor)
% Cell count
Concentration (nM)
WT
March5 KO #1
March5 KO #2
IC50 WT: 4840 nM #1: 813 nM #2: 758 nM
IC50 WT: N/A #1: 20.8 nM #2: 22.7 nM
IC50 WT: 10.0 μM #1: 11.2 μM #2: 13.1 μM
b
Venetoclax
A-1155463
S638845
NEG
dTagV-1
IC50 NEG: 5210 nM dTagV-1: 496 nM
IC50 NEG: N/A dTagV-1: 16.5 nM
IC50 NEG: 5650 nM dTagV-1: 1810 nM
c
Venetoclax (10 μM)
A-1155463 (0.1 μM)
NEG
dTagV-1
Time (h)
C-casp3
Gapdh
d
Venetoclax (10 μM)
A-1155463 (0.1 μM)
Time (h)
Bax
Cytochrome C
Cytosol
Mitochondria
e
Venetoclax
A-1155463
S638845
Empty vector
+Bcl2
+Bcl-XL
+Mcl1
dTagV-1-NEG
dTagV-1
IC50 NEG: 8690 nM dTagV-1: 1720 nM
IC50 NEG: 5080 nM dTagV-1: 14.2 nM
IC50 NEG: 4610 nM dTagV-1: 3770 nM
IC50 NEG: 4290 nM dTagV-1: 18.6 nM
IC50 NEG: N/A dTagV-1: N/A
IC50 NEG: 7780 nM dTagV-1: 5650 nM
IC50 NEG: 5950 nM dTagV-1: 4890 nM
IC50 NEG: N/A dTagV-1:158 nM
IC50 NEG: 4960 nM dTagV-1: 2540 nM
IC50 NEG: 6120 nM dTagV-1:3680 nM
IC50 NEG: N/A dTagV-1:5720 nM
IC50 NEG: 5520 nM dTagV-1: 2160 nM

Fig. 4

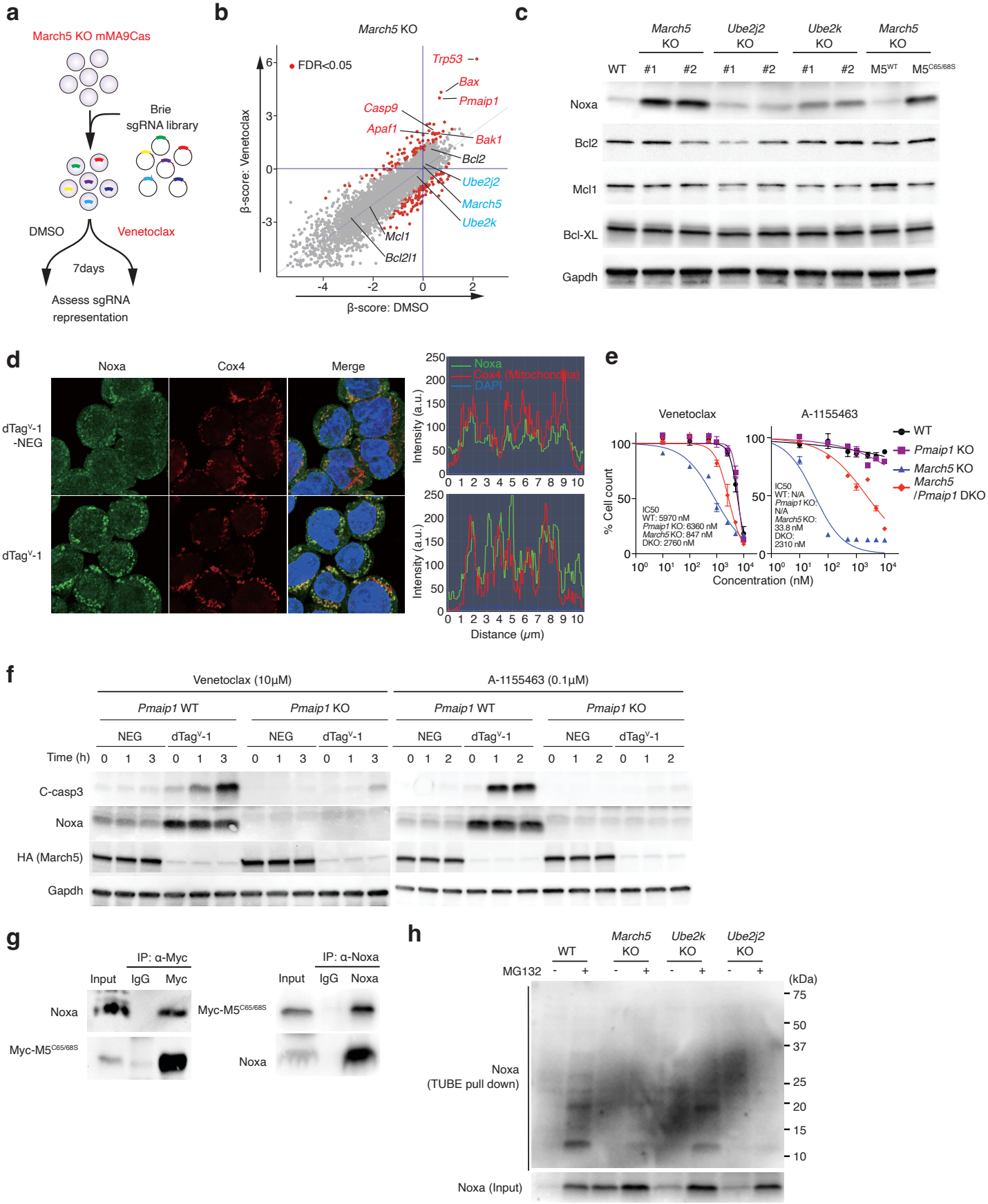
a
March5 KO mMA9Cas
Brie
sgRNA library
DMSO
Venetoclax
7days
Assess sgRNA
representation
b
March5 KO
FDR<0.05
Trp53
Bax
Pmaip1
Casp9
Apaf1
Bak1
Bcl2
Ube2j2
March5
Ube2k
Mcl1
Bcl2l1
β-score: Venetoclax
β-score: DMSO
c
March5 KO
Ube2j2 KO
Ube2k KO
March5 KO
WT
#1
#2
#1
#2
#1
#2
M5WT
M5C65/68S
Noxa
Bcl2
Mcl1
Bcl-XL
Gapdh
d
Noxa
Cox4
Merge
dTagV-1 -NEG
dTagV-1
Noxa
Cox4 (Mitochondria)
DAPI
Intensity (a.u.)
Distance (μm)
e
Venetoclax
A-1155463
% Cell count
Concentration (nM)
IC50
WT: 5970 nM
Pmaip1 KO: 6360 nM
March5 KO: 847 nM
DKO: 2760 nM
IC50
WT: N/A
Pmaip1 KO: N/A
March5 KO: 33.8 nM
DKO: 2310 nM
WT
Pmaip1 KO
March5 KO
March5 /Pmaip1 DKO
f
Venetoclax (10μM)
A-1155463 (0.1μM)
Pmaip1 WT
Pmaip1 KO
NEG
dTagV-1
Time (h)
C-casp3
Noxa
HA (March5)
Gapdh
g
IP: α-Myc
Input
IgG
Myc
Noxa
Myc-M5C65/68S
IP: α-Noxa
Input
IgG
Noxa
Myc-M5C65/68S
Noxa
h
WT
March5 KO
Ube2k KO
Ube2j2 KO
MG132
(kDa)
75
50
37
25
20
15
10
Noxa (TUBE pull down)
Noxa (Input)

Fig. 5

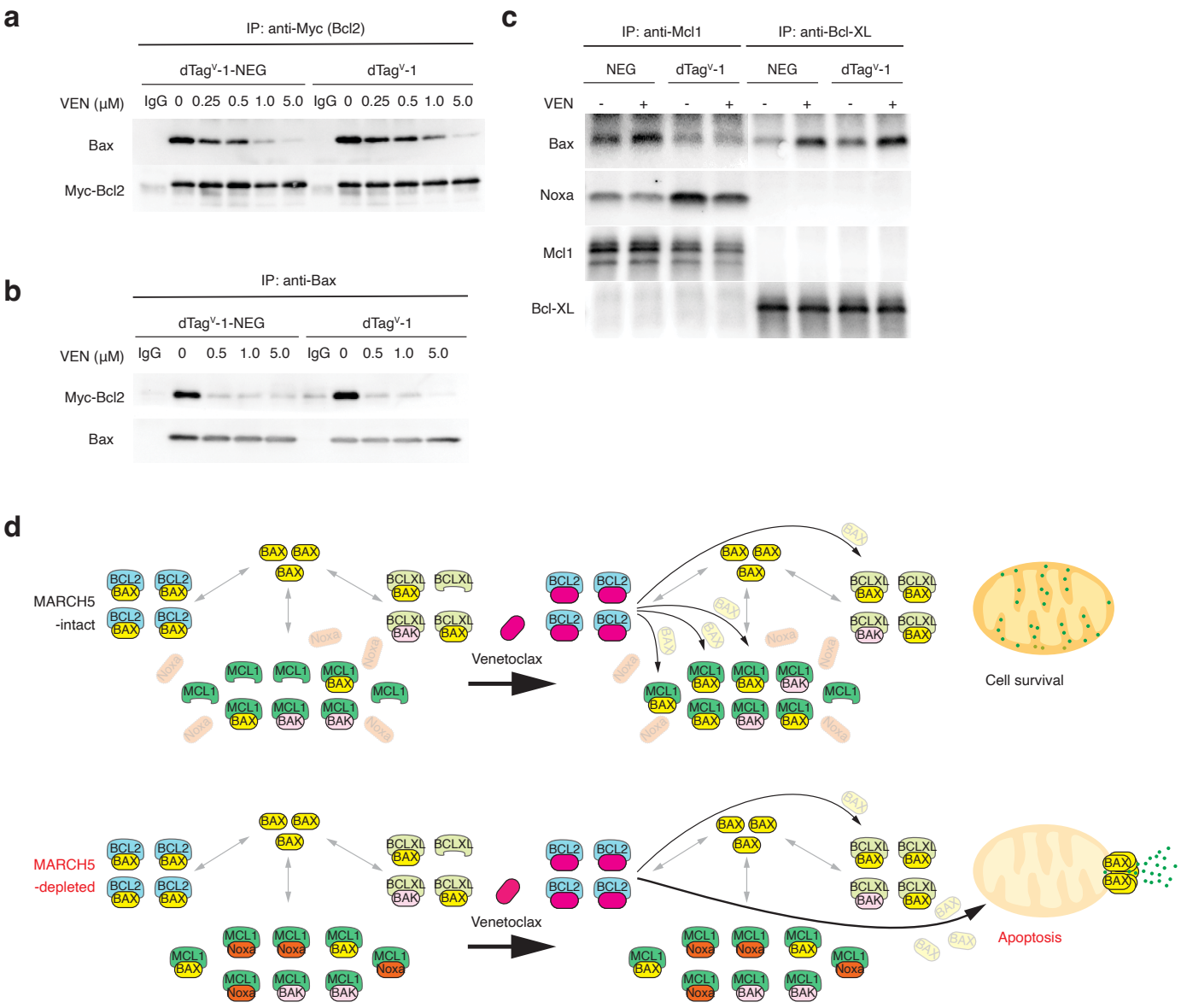
a
IP: anti-Myc (Bcl2)
dTagV-1-NEG
dTagV-1
VEN (μM)
IgG 0 0.25 0.5 1.0 5.0 IgG 0 0.25 0.5 1.0 5.0
Bax
Myc-Bcl2
b
IP: anti-Bax
dTagV-1-NEG
dTagV-1
VEN (μM)
IgG 0 0.5 1.0 5.0 IgG 0 0.5 1.0 5.0
Myc-Bcl2
Bax
c
IP: anti-Mcl1
IP: anti-Bcl-XL
NEG
dTagV-1
NEG
dTagV-1
VEN - + - + - + - +
Bax
Noxa
Mcl1
Bcl-XL
d
MARCH5
-intact
Venetoclax
Cell survival
MARCH5
-depleted
Venetoclax
Apoptosis